Gut dysbiosis was inevitable, but tolerance was not: temporal responses of the murine microbiota that maintain its capacity for butyrate production correlate with sustained antinociception to chronic voluntary morphine

Izabella Sall[a,b,*], Randi Foxall[a,*], Lindsey Felth[c], Soren Maret[a], Zachary Rosa[c], Anirudh Gaur[c], Jennifer Calawa[a,d], Nadia Pavlik [a], Jennifer L. Whistler[c,e,#], and Cheryl A. Whistler[a,#]

[a] Department of Molecular, Cellular, & Biomedical Sciences, University of New Hampshire, Durham, NH, USA.

[b] Graduate program in Molecular and Evolutionary Systems Biology, University of New Hampshire, Durham, NH, USA

[c] Center for Neuroscience, University of California–Davis, Davis, CA, USA.

[d] Microbiology Graduate Program, University of New Hampshire, Durham, NH, USA.

[e] Department of Physiology and Membrane Biology, UC Davis School of Medicine, Davis, CA, USA.

[#]Address correspondence to Cheryl A. Whistler, cheryl.whistler@unh.edu, Jennifer L. Whistler, jlwhistler@ucdavis.edu.

* Contributed equally to this work

Running title: Microbiota Protection from Morphine Tolerance

Key words: Microbiota, opioid, analgesic tolerance, butyrate, short-chain fatty acid, inflammation, dysbiosis, opioid use disorder, morphine.

Word Count: 9501 including in-line reference numbers.

Abstract (197 words)

The therapeutic benefits of opioids are compromised by the development of analgesic tolerance, which necessitates higher dosing for pain management thereby increasing the liability for dependence and addiction. Rodent models indicate opposing roles of the gut microbiota in tolerance: morphine-induced gut dysbiosis exacerbates tolerance, whereas probiotics ameliorate tolerance. Not all individuals develop tolerance which could be influenced by differences in microbiota, and yet no study has capitalized upon this natural variation to identify specific features linked to tolerance. We leveraged this natural variation in a murine model of voluntary oral morphine self-administration to elucidate the mechanisms by which microbiota influences tolerance. Although all mice shared similar and predictive morphine-driven microbiota changes that largely masked informative associations with variability in tolerance, our high-resolution temporal analyses revealed a divergence in the progression of dysbiosis that best explained differences in the development in tolerance. Mice that did not develop tolerance also maintained a higher abundance of taxa capable of producing the short-chain fatty acid (SCFA) butyrate, known to bolster intestinal barriers, suppress inflammation, and promote neuronal homeostasis. Furthermore, dietary butyrate supplementation significantly reduced the development of tolerance. These findings could inform immediate therapies to extend the analgesic efficacy of opioids.

INTRODUCTION

A surge in research has demonstrated the importance of the gut microbiota to host health, leading to the recognition of a gut-microbiota-brain (GMB) axis [1-5]. Whereas the brain influences the gut microbiota by control of gut motility and thereby transit, the microbiota signals the brain via production or modification of neurotransmitters, hormones, microbial byproducts,

and neuroactive metabolites [4, 6, 7]. The gut microbiota are often referred to collectively and nondescriptly as commensals, but many are mutualistic symbionts that support host health. Some others are pathobionts, which are correlated with or capable of causing disease in a context-specific manner. The high load of pro-inflammatory microbial antigens at the microbiota-intestinal mucosa interface produced even by mutualists requires that the host immune responses be trained by the microbiota to be tolerogenic and not over-react, but to still appropriately clear commensals that breach the gut barrier [8]. At this interface mutualistic bacteria enhance local production of anti-inflammatory cytokines to prevent harmful escalation of inflammation.

Paramount among neuroactive signals in the GMB-axis produced by the gut microbiota that maintain homeostasis - balance of gut and host - are various short-chain fatty acids (SCFAs) generated during fermentation of dietary fiber. SCFAs can exert direct local effects by inhibiting host histone deacetylases, thereby epigenetically modifying mucosal immunity to attenuate inflammation, while enhancing gut barriers [9-13]. In addition, as ligands of host G protein-coupled receptors (GPCRs), SCFAs regulate key functions of the gut, including transit and mucus secretion. Upon entering the circulatory system, SCFAs can also signal the brain and other organ axes [6, 11, 12, 14-16]. SCFAs that reach the central nervous system cross and bolster integrity of the blood brain barrier and promote neurogenesis and neuroplasticity [11]. Disruption of signaling cascades contributes to cardio-metabolic and gastric system diseases linked to inflammation and a plethora of neurobiological dysfunctions, including opioid use disorder (OUD) [17-24].

The utility of opioids for treating chronic pain is compromised by the development of tolerance to its analgesic effects, which necessitates dose escalation that can produce physical dependence and place an individual at heightened risk for the development of an OUD. Opioids mediate their effects through activation of Gi-coupled GPCRs, including the primary target of

opioid analgesic drugs, the mu opioid receptor (MOR), which is expressed in the central and peripheral nervous systems, including the enteric nervous system. MORs are also expressed by immune cells, some of which reside in the lamina propria of intestinal mucosa [25]. Many mechanisms have been hypothesized to contribute to analgesic tolerance. Broadly, these fall into two classes: loss of receptor function (receptor desensitization), and homeostatic cellular adaptations that recalibrate baseline signal transduction thereby masking signaling from functional MORs [26]. The processes by which distinct types of MOR-expressing cells adapt to counteract repeated MOR stimulation by chronic opioid likely differ by cell type [26, 27]. Crucially, in MOR-expressing cells such as neurons that transmit sensation, known as nociceptors, the adaptations to chronic opioid drug cause a loss of morphine analgesia, or antinociceptive tolerance to drug (Supplemental Figure 1) [28]. Removal of drug can produce withdrawal effects that include a heightened sensation of pain known as hyperalgesia [29], and severe gastric pain [30]. These rebound effects indicate that, in at least some tolerant states, MORs are present and functioning and that removal of drug unmasks the homeostatic cellular adaptations that produced the tolerance [31]. In humans and even in genetically inbred mice exposed to the same dose of opioid, the degree of antinociceptive tolerance varies, indicating factors beyond genetics or drug exposure contribute to loss of opioid potency [32-34]. Understanding what underlies this variability in response to chronic opioid could produce new mechanistic insight. Preventing or delaying analgesic tolerance would reduce the need for dose escalation, thereby mitigating the risk of overdose and OUD development, and improving the utility of opioids [35].

Through their activation of MORs in the gastrointestinal tract, opioids impair motility and secretion [36, 37] and alter the gut microbiota [12, 38-43]. Gut microbiota dysbiosis is implicated in opioid-induced changes in drug reward [43, 44], dependence [40, 45, 46], hyperalgesia [43, 47], and analgesic tolerance [19, 38, 41]. Several studies document that morphine-induced gut microbiota dysbiosis and subsequent translocation of pathobionts across a morphine-compromised gut barrier trigger inflammation that exacerbates the development of tolerance [27, 35, 41, 48

(Supplemental Figure 2). In agreement with this model, eliminating gut commensals prevents tolerance, and introduction of a common probiotic harboring *Lactobacillus* and *Bifidobacteria* counters inflammation and dysbiosis and slows the development of antinociceptive tolerance as does the use of a peripherally-restricted MOR antagonist [38, 41, 48]. Whether microbiota dysbiosis has a causative effect or tangentially influences tolerance, or if inflammation is the only mediator, is yet unknown and awaits more mechanistic studies.

Importantly, the foundational studies above all minimized and collapsed natural variation in animal and microbiome responses to opioid by using high doses of opioid and aggregating data. Here, we designed a study to leverage both natural variability in degree of antinociceptive tolerance to morphine and microbiota composition with the goal of identifying informative native microbiota signatures that could explain differences in the development of tolerance. We analyzed temporal changes in microbiota abundance, presence, variability, stability and interrogated the potential role of community interactions and metabolic functions [49-52] to expand our understanding of how opioid-induced gut dysbiosis contributes to liability of tolerance. We demonstrated that morphine-induced dysbiosis is inevitable, but tolerance is not. Furthermore, since morphine-induced progressive dysbiosis occurred in all mice, this largely obscured signatures differentiating tolerant from non-tolerant mice that were only discernable by comparative approaches that control for common morphine-induced changes. Whereas tolerant mice shared few distinguishing patterns other than expected higher abundance of pathobionts, mice that did not develop tolerance displayed more shared and predictive features, pointing to a protective role of the microbial neuroactive metabolite butyrate, for preventing the development of tolerance.

MATERIALS AND METHODS

Animals Use and Care

Male wildtype C57/BL6J mice, *mus muculus* (Jackson Laboratory) were used for both the oral morphine paradigm (n=16, 8-week-old; Figure 1 [53]), and subcutaneous (s.c.) morphine paradigm (n=52, 10–11-week-old; Figure 7). An additional cohort of 8 mice (n=4 female and n=4 male) C57/BL6J mice bred in-house at UC Davis were also subjected to the oral morphine paradigm and used as a test dataset for assessing the specificity and accuracy of microbiota associations in prediction models of morphine exposure. All mice had food *ad libitum* and were provided running wheels for enrichment. Mice in oral morphine paradigms had two bottles, one with water and one with morphine, and they were individually housed allowing for the measurement of morphine consumption. Mice in the s.c. morphine paradigm were communally housed (3-4 mice per cage) and had access only to water supplemented with either sodium butyrate (Sigma-Aldrich) or pH-matched (9.30 - 9.50) sodium citrate (EMD) at 100 mM concentration. Bottles containing freshy prepared and filter-sterilized butyrate and citrate were changed every three days for 3-weeks prior morphine exposure and for the duration of the experiment [54]. All procedures involving animals were reviewed and approved by the Institutional Animal Care and Use Committees of the University of California, Davis (IACUC protocol number: 22085) or University of New Hampshire (IACUC protocol number: 230101).

Morphine Administration

For the 18-week oral paradigm (n=16; [53] Figure 1, Figure 2C), mice had access *ad libitum* 5 days per week to both water and water supplemented with morphine sulfate (Mallinckrodt Pharmaceuticals, St. Louis, MO) sweetened with 0.2% saccharin to improve palatability, where the concentration of MS was gradually escalated from 0.3 mg/mL, to 0.5 mg/mL, to a final concentration of 0.75 mg/mL during the first three weeks. Each week, mice then had 2 days where only water was available. Voluntary consumption was determined from bottle weight. Morphine treatment mice in the 9-day s.c. paradigm, received 10 mg/kg of s.c.

morphine sulfate (Cayman Chemical, Ann Arbor, Michigan) in sterile 0.9% saline (Patterson Veterinary Supply, Greeley, CO) (n=36) once each day for 9 days.

Determination of Nociception and Morphine Antinociception

The radiant heat tail flick assay (Tail-flick Meter, Columbus Instruments) was used to assess baseline nociception and morphine antinociception. Light intensity was set to produce baseline of ~2.0 seconds with a cutoff of 6 seconds (for oral paradigm) or 5 seconds (for s.c. paradigm) to minimize tissue damage. Latency was measured without morphine, and then 30 min after morphine injection. For the oral paradigm, mice received 6 mg/kg morphine (ED_{80}) [55] before the study's start and again at the study's completion (Figure 2A). For the s.c. paradigm antinociception was determined on days 1, 7 and 10 at 30 minutes after a 5 mg/kg dose of morphine (ED_{60}), followed by a second dose of + 2 mg/kg morphine (ED_{90}) and a second latency was measured 30 minutes later. Saline control mice (n=16) only received morphine for the antinociception tests (5 mg/kg, and 5+2mg/kg) on day 10. The percent maximum effect (%MPE) was calculated with the following formula: 100 * [(drug response time- baseline latency) / (cutoff time-population baseline latency)]. Dose–responses were evaluated at UNH with 12-week-old male mice to optimize doses for maximum statistical power and effect size using power analysis. These and the cumulative dose responses for evaluating tolerance were fit using GraphPad Prism. The ED_{50} values of the opioid drugs and their 95% confidence intervals were calculated and a shift in AD_{50} from Day 1 to Day 10 was calculated.

Statistical Analysis of Animal Data

Linear regression analyses using Pearson's correlation coefficient [56] determined whether morphine antinociception significantly correlated with total morphine consumption using the R package ggpubr (v0.6.0) [57]. Normality of data was assessed using a Shapiro-Wilk test and homogeneity of variance was assessed using Levene's test. Normality of data was assessed

using a Shapiro-Wilk test and homogeneity of variance was assessed using Levene's test. Data with a p-value greater than 0.05 was considered normal. One-way ANOVA followed by post-hoc analysis using Tukey's Test for multiple comparisons was used to compare differences between groups where assumptions for normality and homogeneity of variance were met. The Kruskal-Wallis test followed by pairwise Wilcox test with corrections for multiple comparisons was used when assumptions of normality and homogeneity of variance were not met. All statistics were conducted using the R package stats (v4.3.0) [58]. Visuals were generated using R 4.2.0 software, GraphPad Prism, BioRender, and some composite figures were modified with Adobe Illustrator.

16S rDNA Library Preparation and Sequencing

Individual mice were placed in clean cages (wiped with 70% ethanol) with no bedding for an hour to defecate normally. Fresh feces were collected and immediately cryopreserved at −80 °C until DNA extraction was performed. Feces were lysed using the Qiagen TissueLyser II (Qiagen, Germantown, MD) for 5 minutes. Microbial genomic DNA was extracted from frozen feces (~100 mg, or 5 pellets) with the ZymoBIOMICS 96 MagBead DNA Kit with lysis tubes (Zymo Research, Irvine, CA), according to manufacturer's protocol. DNA was quantified using the Qubit Quant-iT dsDNA Broad-Range kit (Invitrogen, Life Technologies, Grand Island, NY) using a Tecan M200 plate reader (excitation 480nm/emission 530nm) (Tecan, Männedorf, Switzerland) in a Costar black, clear bottom plate (Corning, Corning, NY). Genomic DNA samples were standardized (11 ng/mL) and freshly diluted to 1.1 ng/mL prior to two-step PCR amplification. The V4-V5 16S variable regions were first amplified in 10 µL reactions in triplicate using the NEB Q5 Hot Start HiFi 2X master mix (New England BioLabs, Ipswich, MA) and 515F and 926R primers as described [59, 60], and modified to include the forward primer pad and linker at the 5' end of each primer. The cycling parameters were as follows: 98°C for 2 min, followed by 22 cycles of 98°C for 10 s, 53°C for 15 s, and 72°C for 15 s, and completing with 72°C for 2

min. Following estimation of size, quality, and quantity of amplicons by gel electrophoresis, pooled amplicons were enzymatically cleaned with ExoSap-IT (Applied Biosystems, Thermo Fisher Scientific, Waltam, MA) and diluted 1:5 in nuclease-free water prior to indexing. In the second step, amplicons were indexed using xGen UDI Primer Pairs (10 mM) in 12 µL reactions using the NEB Q5 Hot Start HiFi 2X master mix (New England BioLabs, Ipswich, MA) with the following parameters: 98°C for 30 s, followed by 10 cycles of 98°C for 10 s, 65°C for 15 s, and 72°C for 20 s, and a final step of 72°C for 2 min. Amplicon band size, quality, and quantity was verified using 2% agarose by gel electrophoresis. Indexed amplicons were pooled in a final library and purified with the Mag-Bind Total Pure NGS kit (Omega Bio-Tek, Norcross, GA). The pooled library was quantified using the Qubit dsDNA High Sensitivity kit (Invitrogen, Life Technologies, Grand Island, NY) and the Qubit 2.0 fluorometer (Invitrogen, Life Technologies, Grand Island, NY). Final amplicon libraries were sequenced and demultiplexed on the Illumina NovaSeq 6000 platform (2 x 250 bp paired end) at the Hubbard Center for Genome Studies at the University of New Hampshire (Durham, NH). Computations were performed on Premise, a central, shared HPC cluster at the University of New Hampshire (Durham, NH) supported by the Research Computing Center and PIs who have contributed compute nodes.

Processing of 16S rDNA Sequencing Reads

All necessary components needed to generate microbial community profiles (e.g., taxonomic assignments, sequence counts, sample metadata, phylogenetic tree;) and to conduct downstream analyses were stored in an experiment-level object using the R package phyloseq (v1.40.0) [61]. For a summary of 16S processing and analysis see Supplemental Figure 3.

Amplicon sequencing primers were removed from demultiplexed sequencing reads using the cutadapt plugin [62] in the QIIME 2 2020.2 pipeline [63] before being processed using the R package DADA2 (v1.18) quality control pipeline [64] and custom scripts for post-processing artifact removal. Taxonomy was assigned using the GreenGenes reference database (v13.8) [65].

Species, where applicable, were identified using rRNA/ITS databases with the nucleotide basic local alignment search tool (blastn) [66]. A taxonomic filter was applied to remove unclassified phyla, chloroplasts, and mitochondria, along with an additional abundance filter to remove singletons and doubletons from the dataset (phyloseq v1.40.0) [61]. Maximum likelihood phylogenetic trees with bootstraps were estimated from MAFFT (v7.305b) [67, 68] alignments using RAxML (v8.2.10) [69], followed by tip-agglomeration (h = 0.5) to combine similar amplicon sequence variants (ASVs) into one representative taxon sequence or taxa agglomeration to the genus level using phyloseq (v1.40.0) [61]. Sequencing counts were transformed to relative abundances (phyloseq v1.40.0) [61] or normalized to center-log ratios (R package microbiome v1.18.0) [70].

The presence of batch effects that may introduce bias were assessed by comparing sequenced controls using the R package MMUPHin (v1.10.0) [71] and principal coordinates analyses (PCoA). The controls used to assess bias included 1) a ZymoBIOMICS Microbial Community Standard II (Log Distribution) to detect any bias introduced during DNA extraction, 2) a ZymoBIOMICS Microbial Community DNA Standard II (Log Distribution) to detect any bias introduced during amplification, 3) a randomized representative mouse fecal sample to detect any bias introduced from multiple sequencing runs, and 4) a no template mock DNA extraction to capture any potential contaminants.

Analysis of Microbiota Diversity

Overall gut microbiota diversity and temporal changes assessed by weighted UniFrac [72], unweighted UniFrac [73] (membership), and Bray-Curtis dissimilarity (relative abundance) was analyzed using PCoA. Permutation Multivariate Analysis of Variance (PERMANOVA) tests [74] determined any statistical differences between experiences and the development of antinociceptive tolerance throughout the paradigm using the permanova_pairwise function in the R package ecole (v0.9-2021) [75]. Prior to using PERMANOVA, pairwise permutation tests [76, 77]

for homogeneity of multivariate dispersion [78-80] determined any statistical differences in group variances of experiences and the development of antinociceptive tolerance throughout the paradigm using the betadisper and permutest functions in the R package vegan (v2.6-4) [81]. All visuals and statistical analyses were generated using R 4.2.0 software.

Alpha-diversity of non-tolerant and tolerant gut microbiota were analyzed using the estimate_richness function for Shannon diversity in the R package phyloseq (v1.40.0) [61]. Average alpha-diversity and standard errors were plotted sequentially and abrupt variations over time that may represent key transitions were detected using a Bayesian analysis of change point in the R package bcp (v4.0.3) [40, 82], which implements the Barry and Hartigan product partition model for the standard change point problem using Markov Chain Monte Carlo [83]. Timepoints with a posterior probability of change in the mean abundance greater than 0.70 of community members in tolerant or non-tolerant mice were marked on time series plots.

Differential Abundance and Biomarker Analyses

Community members, grouped at the genus level, that were different in abundance between tolerant and non-tolerant mice, and between pre-, during, and post-morphine exposure phases of the paradigm, were determined using the differential test within the R package corncob (v0.3.1) [84]. Non-normalized counts were used with the Wald setting within the differential test to distinguish community members associated with the covariate of interest controlling only for sequencing run and phase of morphine. The count abundance for each genus was fit to a beta-binomial model using the logit link functions for both the mean and overdispersion simultaneously. The null and non-null overdispersion models were specified with the same confounding variables (paradigm experience and sequencing plate) to identify only genera having differential abundances associated with the covariate of interest. The list of differentially abundant and/or variable community members produced was further analyzed

using linear discrimination analyses of effect size (LEfSe Galaxy v1.0) [85] to identify any community members that most likely explain differences between aa covariate of interest.

Indicator Species and Prediction Models

We used an indicator species analysis to determine community members unique to experiences and to provide evidence for the impacts of experience on the gut microbiota [86]. Furthermore, we tested whether there were combinations of up to 3 indicator species that could predict whether a sample was from a morphine exposed gut microbiota. Abundance data for the cohort was transformed into presence absence data and indicator value analysis with experience as the grouping (pre-morphine, morphine, post-morphine) was performed using the multipatt() function with 999 permutations in the R package indicspecies [86]. To determine which combinations of community members could best predict whether a sample was from morphine exposure we reduced the dataset to samples that were from pre-morphine or mid-late morphine and used the indictors() function with up to 3 combinations of community members, and subsequently the pruneindictors() function to assess which combinations were best predictors. Next, we tested whether the combinations which were only found in mid-late morphine samples (Probability A=1) could accurately predict which samples were most likely from morphine exposed microbiota from a separate cohort of 8 animals (n=4 female, n=4 male) that consisted of 40 pre-morphine, 102 morphine samples, and 15 post-morphine samples.

Longitudinal Change Point Analysis

Abrupt variations over time that may represent key transitions in community members that were differentially abundant between tolerant and non-tolerant mice were detected using a Bayesian analysis of change point in the R package bcp (v4.0.3) [40, 82], which implements the Barry and Hartigan product partition model for the standard change point problem using Markov Chain Monte Carlo [83]. Timepoints with a posterior probability of change in the mean abundance

greater than 0.790 of community members in tolerant or non-tolerant mice were marked on time series plots.

Analysis of Temporal Stability

The temporal stability of populations (All ASVs, grouped at the genus level) exposed to morphine was evaluated and visualized within the context of Taylor's power law, which describes the ubiquitous macroecological relationships between the mean and variance of an individual taxon [87]. Two extensions of this law were used to examine whether the microbiota of tolerant and non-tolerant mice differ in variability or stability. The Type I power law extension was used to detect differences in temporal variability of tolerant and non-tolerant microbiota across all phases of morphine experience and the Type IV power law extension was used to examine differences in microbiota stability relative to starting composition at each phase of morphine experience [88]. When applying the Type IV extension, Taylor's power law which is described by the formula $V = aM^b$, where V is the variance, a is a scalar parameter, M is the mean, and b is an exponential parameter, the formula was log-transformed, $\ln(V) = b\ln(M) + \ln(a)$, where b is the slope parameter [88, 89]. The exponential/slope parameter b of the Type IV power law extension was standardized by subtracting the mean b of all individuals pre-morphine from each individual mouse's value for b at each morphine experience to produce the change in slope. Positive values of the slope parameter b represent instability, whereas 0 or negative values of the slope parameter b represent stability relative to pre-morphine.

Microbiome Association Networks

Microbial association networks were inferred from the gut microbiomes of mice before entering the self-administration of oral morphine phase in the paradigm compared to the gut microbiomes after 18-weeks of morphine administration to 1 week post administration. Community members were grouped at the genus level using the tax_glom function from

phyloseq (v1.40.0) [61]. Seventy out of 165 taxa grouped at the genus level were at the highest frequency. SPRING associations were measured in the gut microbiota split by whether they were taken before or after morphine exposure and another iteration where microbiota were split based on development of antinociceptive tolerance. Microbial association networks for each group were inferred using the signed distance, nlambda, and rep.num (100) functions in the R package NetCoMi (v1.1.0) [90]. For reproducibility, microbial association network analyses used the random seed "12345". Differential networks were inferred from SPRING association networks using fisher test adjusting for false discovery rate.

Analysis of Predicted Functional Profiles

Functional profiles of gut microbiota from tolerant and non-tolerant mice were predicted from representative ASVs of 16S rDNA sequences using phylogenetic investigation of communities by reconstruction of unobserved states (PICRUSt 2.0) pipeline [91]. Gene content, represented by Enzyme Classification (EC) numbers, (i.e., gene family copy numbers of ASVs and abundances per sample) per ASV was predicted [92] by aligning ASVs to reference sequences and placement into a reference phylogenetic tree [93-95]. MetaCyc functional pathways and associated abundance were inferred from EC number abundances [96]. Differential abundance testing of functional pathways between tolerant and non-tolerant mice was analyzed and visualized using the R package ggpicrust2 (v1.7.3) [97].

RESULTS

Not all mice developed antinociceptive tolerance to chronic morphine

To examine variables that contribute to differences in OUD liability, particularly antinociceptive tolerance to morphine, individually housed wild-type mice underwent an 18-week longitudinal paradigm of voluntary oral morphine self-administration, where they had *ad*

libitum access to both morphine and water [53]. To determine the development of tolerance, we used reflexive tail-flick to radiant heat to measure nociception -the ability to sense- and antinociception -the ability of morphine to block sensation- with a non-contingent morphine dose (6 mg/kg, s.c.) at the start and end of the self-administration paradigm (Figure 1A). Mice in this paradigm displayed variability in day 0 baseline morphine antinociception and in tolerance to antinociception after 18-weeks of morphine self-administration (Figure 1B). More than a third of mice (6/16) maintained 100% of the maximum possible effect (MPE) to morphine antinociception (i.e. non-tolerant) after 18-weeks of chronic exposure. As a population, after 18-weeks of chronic morphine, mice in our paradigm did not display a significant decrease in baseline nociceptive threshold in the absence of morphine (i.e. hyperalgesia), despite consuming, on average, 25 mg/kg of morphine daily (range of 5-120 mg/kg daily; Figure 1C & Supplemental Figure 4). For most individual mice, tolerance to morphine (e.g. decreased %MPE) did not correlate with a change in baseline nociceptive threshold in the absence of morphine indicating that tolerance was not driven solely by hyperalgesia (Supplemental Figure 4B). Importantly, individual variation in morphine tolerance also did not correlate with the amount of morphine consumed (Figure 1C), indicating that variables beyond degree of drug intake influenced the development of tolerance. Individual pre-morphine microbiota, as determined from 16S rRNA libraries generated from feces, was highly variable (Figure 1D, $p_{\text{PERMANOVA}} = 0.0001$) even though the mice were the same age, sex, inbred genotype, and from the same commercial source. This led us to hypothesize that holobiont genetic variation in the form of the hosts' starting microbiome and/or its response to morphine might explain differences in the development of antinociceptive tolerance.

Morphine induced progressive dysbiosis in all mice regardless of whether they did or did not develop tolerance

We capitalized upon our unique experimental design of intensive sampling to map the temporal impact of morphine on gut microbiota, thereby capturing snapshots of mouse guts at different phases of morphine experience. We then evaluated whether differences in microbiota were associated with variability in tolerance (Figure 2 and Supplemental Figure 5; details provided in Supplemental Tables 1 & 2). Preliminary exploration of microbiota using Bray-Curtis dissimilarity of all amplicon sequence variants (ASVs) demonstrated how morphine caused progressive shifts in bacterial community assemblages ($p_{\text{PERMANOVA}} \leq 0.01$ for all pair-wise comparisons), even in mice that did not develop antinociceptive tolerance to morphine (Figure 2A). The microbiomes of tolerant and non-tolerant mice did not form separate clusters at any phase of the paradigm, and because of this, it is apparent that the experience of morphine was the primary driver of microbial communities (Figure 2A and Supplemental Figure 5). We also investigated whether morphine increased variability as a dimension of dysbiosis (Supplemental Figure 6). Early morphine exposure increased the number of variable genera relative to pre-morphine, and as morphine exposure continued, the number of variable genera increased again later in the paradigm and remained variable even post-morphine.

To further visualize dysbiosis, we examined how global network properties and differential networks of microbiota were impacted by morphine, as context for identifying differences between tolerant and non-tolerant mice [90]. Comparisons of high-level relationships revealed that the connections among the most central nodes that represent keystone species (community members that connect the most community members) were significantly weaker and at times eliminated by chronic morphine, but these changes were not driven by individual genera within each central node (Figure 2B, detailed in Supplemental Table 3). Subsequent examination of pair-wise community member associations from these networks further reflected how morphine weakened or caused a loss of many associations (Supplemental Table 3). One positive association between two potential pathobionts, *Desulfovibrionaceae* and *Bacteroidales,*

became stronger and one association between related Gram-positive taxa, an unclassified member of family *Erysipelotrichaceae* and genus *Coprobacillus,* was gained.

Since morphine experience in the paradigm appears to be a strong driver of microbiome assemblages, we evaluated whether morphine-driven disturbances were predictive of morphine use thereby strengthening inferences from microbiota associations. We did this by determining how well combinations of associated taxa identified from our experimental cohort could distinguish between pre-morphine versus morphine-treated microbiota from a different cohort of mice that experienced the same self-administration paradigm (Figure 1A). To evaluate this, we trained models on 30,295 different combinations of up to 3 community members associated with mid- to late morphine with our experimental cohort of mice (bred at Jackson Laboratory, JAX). We then tested these models on microbiota from a second cohort of mice bred in-house (n=4 female, n=4 male) (Figure 2C, data and statistics summarized in Supplemental Table 5 & 6). Even though the starting composition of the two experimental cohorts differed substantially likely reflecting breeding facility, predictive models using the top eight ranking community profiles accurately identified most pre-morphine microbiota (Figure 2C). Furthermore, the models also had similar predictive power on all morphine-exposed microbiota of the home-bred mice compared to JAX-bred mice (46% as opposed to 57%). The robustness of the models across independent experiments throughout the paradigm suggests that nuances in starting microbiota composition did not strongly impact global morphine-induced compositional changes, even those that were sustained after morphine was removed, and that morphine induced common, predictive changes in the microbiota. This also exemplifies how co-occurrence indicator analyses could prove useful for identifying morphine use.

Morphine concurrently depleted mutualistic community members that support gut homeostasis and increased relative abundance of pathobionts.

Using taxonomic assignments, we identified the genera that were altered by morphine and best explained differences between pre- and morphine-exposed microbiota, representing biomarkers of morphine exposure [84]. We then visualized temporal changes in their abundance during the different phases of morphine experience compared to pre-morphine to glean insight into the dynamics that explain morphine dysbiosis (Figure 3A). Among 33 taxa identified as biomarkers, most were depleted by morphine and only emerged after prolonged morphine exposure. Fewer taxa increased in abundance with morphine exposure (Figure 3A). All biomarker taxa were also differentially variable in response to morphine (e.g. Supplemental Figure 6).

Congruent with the expectation of morphine-driven dysbiosis, some pathobionts, including *Allobaculum, Prevotella, Erysipelotrichaceae,* and *Streptococcus* [98-103], increased in abundance with morphine treatment, whereas some potential mutualistic taxa, including *Akkermansia*, *Bacteroides, Clostridium,* and *Rosburia* [27, 104, 105] decreased in abundance (Figure 3B, Supplemental Table 3). Notably, many of the microbiota depleted by morphine are associated with gut barrier integrity, and/or are predicted SCFA-producing taxa [27, 106-110] (Figure 3B, Supplemental Tables 6 & 7). Though these beneficial genera trended towards a gradual depletion, some beneficial genera increased in abundance at times, including *Clostridium, Parabacteroides, Lactobacillus* and *Blautia* [106, 111, 112] (Figure 3A, Supplemental Table 6 & 7).

Collectively, these analyses highlight the significant, progressing, and enduring effects of prolonged morphine use, where the microbiota did not return to its pre-morphine exposure state, at least not within the several weeks after morphine was removed (see Figure 1A for paradigm details). These changes also align well with mounting evidence that morphine-driven dysbiosis precipitates tolerance via pathobiont overgrowth which has the potential to trigger uncontrolled inflammation due to loss of commensals that help to attenuate this inflammatory response (Supplemental figure 2) [12, 38-43]. However, morphine produced significant, progressing dysbiosis

in all mice, even those that did not develop tolerance and, as such, tolerance cannot be explained simply by these global changes. We posited that if nuanced differences in the responses of the microbiota contributed to differences in the development of tolerance, they would likely be overshadowed unless the analyses accounted for the common morphine experience through time.

Tolerant mice exhibited earlier microbiota instability and depletion of beneficial taxa

Even with the dominating morphine-induced dysbiosis in all mice, there were clues that morphine disturbed the microbiota differently in tolerant and non-tolerant mice. We explored this potential using a Bayesian methodology to examine change-points in α-diversity. This analysis revealed a significant decrease in count and balance of ASVs and this occurred earlier, by week 5 of morphine exposure in tolerant mice, as opposed to week 9 in non-tolerant mice (Figure 4A). Analysis of β-diversity also revealed that the microbiota of tolerant and non-tolerant mice differed in membership and abundance during morphine consumption ($p_{\text{PERMANOVA}}$ = 0.0022, weighted UniFrac), though diversity did not differ either before or after morphine (Supplemental Table 1). These results suggest a link between the progression of microbiome dysbiosis and the difference in tolerance. The dramatic drop in diversity identified in tolerant microbiota were detected during the mid-morphine phase of exposure but may have resulted from an earlier loss of stabilizing community members, as evidenced by divergences in diversity during the early morphine phase of exposure (Figure. 4A).

We next identified differentially abundant genera associated with the development of tolerance/protection from tolerance using a beta-binomial regression model to control for phase of morphine experience [84]. From among these genera, we identified biomarkers- genera that are significantly correlated with and most explained the difference between tolerant and non-tolerant

mice [85]. These analyses revealed relatively few biomarkers, eight for tolerant mice and 11 for non-tolerant mice (Figure 4B, see Supplemental Table 8 for details and statistics). Three genera, all recognized as "probiotic," were biomarkers before morphine exposure. Specifically, tolerant mice initially harbored higher abundances of *Lactobacillus* and *Bifidobacterium,* whereas non-tolerant mice exhibited higher abundances of *Akkermansia muciniphila* (Figure 4B). Although *A. muciniphila* increased after morphine exposure even in tolerant mice, a higher level was maintained longer in non-tolerant mice (Figure 4B, Supplemental Figure 7). Earlier changepoints, or periods of instability, led to some divergent patterns of abundance in tolerant versus non-tolerant mice, including higher abundance of pathobiotic genera *Desulfovibrio* and *Coriobacteracea*, and lower abundance of potentially beneficial taxa *Rickenellaceae* AF12 and *Odoribacter* in tolerant mice (Figure 4B, Supplemental Figure 7).

Most biomarkers were only apparent after morphine had substantially altered microbiota composition, with notable exceptions (e.g. *A. muciniphila*), but this does not preclude that individual microbiota differences earlier in the paradigm, or even prior to morphine exposure, impacted antinociception and/or the trajectory of morphine tolerance. For example, four mice exhibited low morphine antinociception prior to chronic morphine consumption and antinociception was further compromised by chronic morphine (Figure 1B, colored mice). The most noteworthy difference between the pre-morphine microbiota of mice with high and low starting antinociception was the near absence of *Odoribacter* [113] in mice with low starting antinociception (Supplemental Figure 8; detailed statistics in Supplemental Table 9).

We also assessed the stability of the gut microbiota of individual mice as a measure of dysbiosis, and assessed whether the two populations- tolerant and non-tolerant mice- met the expectations of Taylor's power law [87, 114, 115]. Taylor's power law describes the scalable relationship between the variance in abundance of a taxon to their population mean and it can be used to explore ecologically meaningful differences in population dynamics that result from

external drivers and interactions among different taxa [88, 116]. Application of the Type I power law extension [88] showed an expected correlation of variance of individual genera with their population means regardless of phase of morphine experience and development of tolerance as demonstrated by significant aggregation and linear clustering of data (Supplemental Figure 9). However, application of the Type IV power law extension, which examines individual communities over time [88], detected differences in temporal stability between microbiota from tolerant and non-tolerant mice (Figure 4C, see methods for details). Specifically, the slope parameter of microbiota from tolerant mice increased (positive value) during mid-morphine indicating greater variance relative to starting variance, a result that was not driven by any one individual. In contrast, the slope parameter of microbiota from non-tolerant mice did not increase (0 or negative value). The increase in population variance in tolerant mice indicates temporal instability among these populations (Figure 4C). Importantly, this trend coincides with the change in α-diversity observed in tolerant mice at week 5 of the paradigm (Figure 4A).

Since morphine significantly altered relationships of the most central community members in all mice (Figure 2D), we wondered whether the relationships of microbiota of mice that did or did not develop tolerance differed [90]. Overall microbiota connectivity did not differ between tolerant and non-tolerant mice, further reinforcing that all mice experienced dysbiosis (Supplemental Figure 10). However, network differences between tolerant and non-tolerant mice were revealed by an assessment of whether the abundance of paired community members correlated with each other and were different in the two populations (Figure 4D, Supplemental Table 10). This analysis identified six stronger positive associations and two unique negative (inverse) correlations in mice that did not develop tolerance, and four positive associations and one negative correlation that were unique to tolerant mice.

We also interrogated whether patterns in unique membership, or indicator genera were linked to tolerance [86]. Only three taxa altered by morphine were differentially present in tolerant

mice, and these were identified late and post-morphine or when all phases of morphine experience were combined (Table 1). In contrast, nine indicator taxa were identified from non-tolerant mice, some from every phase of morphine experience (Table 1). With the exceptions of *Odoribacter, Rickenellacea AF12, and Flexispira*, which are indicators of non-tolerance, and *Rhodococcus*, an indicator of tolerance, all indicator taxa were significantly impacted by morphine in terms of abundance (Figure 3A, Supplemental Table 2), as indicator species (Supplemental Table 4), or changes in network centrality (Figure 2C, Supplemental Table 3). *Bilophilia* was an indicator of both tolerance and morphine. *Streptococcus* was both an indicator of tolerance and displayed a unique network association in tolerant mice (Table 1, Supplemental Table 2, Supplemental Table 4).

Genera differentially associated with non-tolerant mice were more predictive and stably maintained during morphine disturbance than genera associated with tolerant mice

To further examine the strength and patterns of microbiota associations with differences in the development of tolerance, we applied predictive models of abundance and presence of up to 3 community members identified at each phase of morphine experience in association with either tolerant or non-tolerant mice [86](Summarized in Figure 5 and Supplemental Table 11, see Supplemental Table 12 for a full description models and statistics). Starting composition was not predictive of either population, in agreement with individual variability of pre-morphine microbiota (Figure 1D, Supplemental Figure 5), similar alpha and beta diversity, (e.g. Figure 4A) and the limited number of biomarkers identified pre-morphine (Figure 4B). The models built from early morphine associations were more specific for tolerant microbiota and assigned these with 100% accuracy, as opposed to only 83% accuracy for non-tolerant mice indicating distinguishing changes were occurring in the microbiota of tolerant mice even during early morphine. Whereas the number and predictive capacity of tolerant and non-tolerant models

were similar mid-morphine, this shifted late morphine where more models could predict microbiota from tolerant as opposed to non-tolerant mice (seven versus four). Finally, by post-morphine all models assigned microbiota from individual fecal samples to the tolerant and non-tolerant groups with 100% accuracy reflecting that the microbiota were divergent. There were, however, more models (eight versus three) predictive of non-tolerant than tolerant microbiota (Supplemental Table 12).

A visual exploration of the temporal distribution of the genera that informed these predictive models reveals that many genera predictive of non-tolerant microbiota spanned multiple phases of morphine experience, reflecting their stable association (Figure 5). In keeping with this, when statistically supported ($p < 0.05$) models built with genera associated with non-tolerant or tolerant microbiota at discrete phases of morphine exposure were applied to all microbiota samples, regardless of the phase from which they were collected, the non-tolerant microbiota models had more cross predictability (68% of non-tolerant samples correctly identified versus 57% tolerant samples). Collectively, this data supports that microbiota from tolerant mice were more temporally unstable and more divergent from each other than the microbiota of non-tolerant mice. This is perhaps not surprising considering non-tolerant mice did not vary in antinociception, whereas tolerant mice varied more from one other (Figure 1B). But the cross-predictability between the microbiota of just 6 non-tolerant mice suggests a convergence in mechanisms of sustained antinociception as well as resistance to some morphine-driven changes (Figure 4).

Considering tolerant mice appear less alike each other and non-tolerant mice appear more convergent in shared and predictive genera, we re-evaluated similarity among microbiota that were from tolerant or non-tolerant mice and differences between these two populations using only biomarker genera and a phylogenetically informed metric of β-diversity (weighted UniFrac) (Supplemental Figure 11). This analysis indicated that phase of morphine experience

was still the major driver of assemblages, even when considering a restricted dataset (19 ASVs at the genus level). In addition, this analysis revealed more variability among the microbiomes of tolerant mice than non-tolerant mice during mid-morphine (Supplemental Figure 11). This agrees with the timing in which we predicted community instability in tolerant mice (Figure 4C) following their notable earlier changepoint in α-diversity (Figure 4A) as well as application of Taylor's power law (Figure 4C). In contrast, microbiota of non-tolerant mice clustered more tightly mid-morphine, suggesting more similarity and perhaps shared functions (Supplemental Figure 11).

Preservation of butyrate-producing genera was associated with non-tolerant mice, and supplementation with butyrate protected against the development of tolerance to morphine.

The finding that mice that did not develop tolerance to morphine share more predictive genera and associations were still quite different from each other in terms of community structure even when only considering biomarker genera (Figure 5, Supplemental Figure 11, and Supplemental Table 12) led us to consider whether functions could elucidate what these mice have in common. Assessment of previously described attributes of biomarker and indicator genera revealed a striking pattern among genera associated with non-tolerant mice: a higher abundance and association of butyrate producers that was corroborated by a bioinformatic analysis that predicts the functional capacity of taxa (Table 2, Supplemental Figure 12). Congruent with this observation, butyrate bolsters gut barrier function, curtails inflammatory responses while stimulating macrophage differentiation to remove invading pathobionts, and promotes gut homeostasis [159, 160]. It is notable that many of the butyrate producing genera associated with non-tolerant mice were also lower in mice with poor starting antinociception prior to morphine exposure and some were subsequently depleted even more by morphine, in

parallel with the further decline of morphine antinociception in these mice (Figure 1B, Supplemental Figure 8). This suggests that morphine-driven differential loss of some butyrate-producing organisms might exacerbate tolerance and by extension that butyrate could protect against tolerance (Supplemental Figure 2).

To investigate whether butyrate reduces the degree of tolerance, we optimized a paradigm that uses a moderate exposure of s.c. morphine to gradually but reliably produce tolerance in most mice while preserving variation in microbiota response to morphine and some variation in degree of morphine tolerance. We then used this paradigm to evaluate the impact of butyrate on tolerance. Mice were supplied with sodium butyrate, or as a control sodium/pH-matched sodium citrate, a common food additive, *ad libitum* in their drinking water for three weeks prior to morphine exposure. Day 1 latencies to tail flick without morphine, and with morphine at 5 mg/kg (ED_{60}), and 5+2 mg/kg (ED_{90}) did not differ between butyrate and citrate supplemented mice (Supplemental Figure 13A, B). However, only one butyrate mouse (~6%) was below 100% MPE at the ED_{90} morphine dose as opposed to four citrate mice (~22%). This implies butyrate pretreatment may modestly bolster morphine antinociception. Mice were then treated with non-contingent morphine (10 mg/kg s.c. 1x day for 9 days) or saline while continuing to receive butyrate or citrate supplementation (Figure 6A). On day 10, the baseline nociception of the morphine treated mice in the two supplementation groups did not differ from their respective saline control groups and few individuals exhibited a change in nociception (Supplemental Figure 13C). However, morphine-mediated antinociception declined precipitously in citrate-supplemented mice, and as a population only citrate-supplemented mice were tolerant by day 7 (Figure 6B). Furthermore, on day 10, butyrate-supplemented mice maintained significantly higher morphine antinociception than citrate mice (Figure 6C). More specifically, only citrate-supplemented mice exhibited a significant decline in morphine potency from ED_{50} of 5.3mg/kg to 8.1 mg/kg ($p=0.016$), whereas the butyrate-supplemented mice did not exhibit a significant decrease in morphine potency (from ED_{50} 5.2 mg/kg to 6 mg/kg, $p=0.60$) (Figure 6D).

DISCUSSION

Prior studies examining contributions of the microbiome to OUD have intentionally reduced behavioral variation inherent to mouse models by using high non-contingent morphine doses. These prior studies have thereby gleaned insight from common microbiome responses not all of which are likely to explain tolerance [19, 38, 41]. In contrast, through our experimental design, here we preserved and leveraged natural variation in tolerance and the microbiota with the specific goal to identify microbiota signatures associated with degree of tolerance (Figure 1 and 6). We demonstrated that chronic voluntary morphine self-administration induced similar, even predictive, dysbiosis in all mice, regardless of whether they develop antinociceptive tolerance (Figure 3A, Table 1) and these global changes largely masked informative microbiome associations that tracked with differences in morphine tolerance. To uncover latent patterns associated with tolerance, we used complimentary high resolution temporal analyses and cross-referenced results to identify repetitive trends. These analyses revealed a divergence in the timing of progression of dysbiosis between tolerant and non-tolerant mice (Figure 4). More importantly, there were noteworthy differences in the response of microbiota to morphine disturbance that best distinguished between mice that did and did not develop tolerance (Figure 4, Figure 5, Table 2). Key among these findings was that non-tolerant mice maintained higher abundances of producers of butyrate, a ligand of communication in the GMB-axis which is also known to bolster barrier function and suppress inflammation (Table 2)[8, 161]. We subsequently showed that diet supplementation with butyrate protected against the development of tolerance to morphine (Figure 6). This study implicates butyrate production is a potent protective tool of the microbiota that may counter adverse effects of morphine that disrupt the normal communication along the GMB-axis (Figure 6; Supplemental Figure 2, Supplemental Figure 14).

As researchers increasingly recognize the importance of the gut microbiota and its signaling through the GMB-axis to host health and disease [1-4], there has been a shift in thinking about how hosts and their associated microbial communities, known as the holobiont, interact

to influence individual phenotypes [162-164]. Prior studies suggest that the gut microbiota enhances morphine tolerance through its translocation across a morphine-compromised gut barrier, as tolerance can be reduced by elimination of the gut microbiota via antibiotics, or in germ free mice [38, 41, 99]. The implication that the microbiota is the problem paints an incomplete picture, especially considering that depletion of gut mutualists, and their supportive functions, is arguably the most apparent feature of morphine-induced dysbiosis (Figure 3) [132]. Furthermore, a diverse gut microbiota is crucial for both immune and neurological functions [3, 165-167]. Indeed, supplementation with a probiotic mix of *Lactobacillus* and *Bifidobacteria*, gram positive genera shown to be depleted by morphine [39, 40, 42], improves barrier integrity and attenuates morphine tolerance [41]. Oddly enough, higher populations of these same genera were biomarkers of tolerance in our study here (Figure 4B) and *Lactobacillus* modestly increased in response to morphine in tolerant but not in non-tolerant mice (Figure 3A). Depletion of gram-positive bacteria with vancomycin, which targets and depletes these probiotic genera also prevents morphine tolerance [38]. We expect this incongruence, whereby these beneficial genera are tied to both tolerance and its attenuation, could reflect that a variety of taxa, not just these two genera, can bolster gut integrity similarly and support trophic networks of the microbiota to resist or counter morphine's adverse effects (Figure 2D, Table 2). Importantly, these capabilities may not necessarily be defined by or limited to related taxa, or even guaranteed to be expressed equally by every strain within a given species (Supplemental Figure 8 and Table 2; [168, 169]. Functional redundancy of SCFA production by the microbiota could ensure resiliency to perturbation [170-173].

Among SCFAs, which include acetate, propionate, and valerate, butyrate is especially important in the intestinal environment as the primary energy source for colonocytes. Butyrate both promotes barrier function and modifies immune responses to clear commensals that breach the gut barrier while also curtailing damaging inflammation before it escalates to cause systemic harm (Supplemental Figure 14)[159-161, 174, 175]. Notable potential butyrate producers

associated with non-tolerance included *Oscillospira*, *Coprococcus*, *Parabacteriodes*, *Anaerofustis*, *Odoribacter, and Rickenellacea AF12,* (Table 2) [106, 110, 111, 113, 137, 141, 148, 176-181]. Many of these genera have been shown to improve gut integrity and inversely correlate with inflammatory conditions such as inflammatory bowel disease, cardio-metabolic diseases, and neurobiological or neurodegenerative conditions [110, 111, 113, 119, 130, 137, 176, 182-187]. The replication of protection from tolerance by diet supplementation of butyrate alone (Figure 6) suggests a mechanism by which the identified taxa could exert their effects and could explain why differential loss of such community members could lead to cytokine-directed inflammation that is a suggested cause of opioid-induced hyperalgesia and tolerance [19, 38, 41, 175] (Supplemental Figure 14), though it does not dictate that other mechanisms are not at play. One possibility is that butyrate palliatively countered the reduced analgesic benefits of morphine as tolerance developed by changing the threshold of pain perception by attenuating inflammation, thereby preventing pain sensitization of nociceptor neurons, rather than preventing homeostatic adaptations from occurring [41, 188] (Figure 7; Supplemental Figure 14). This aligns with a recent study showing butyrate protection from hyperalgesia [47]. However, the development of tolerance in our paradigm did not require hyperalgesia (Supplemental Figure 4; Supplemental Figure 13C, D), and four mice with naturally lower levels of some butyrate producers (e.g. *Odoribacter*) displayed deficits in morphine antinociception akin to tolerance even before chronic morphine caused dysbiosis and drove the development of tolerance (Supplemental Figure 8; Table 2).

As a complementary mechanism to its documented ability to reduce gut and neuro-inflammation, butyrate could have modulatory effects on neuronal activity directly. The gut is innervated by both enteric and sensory nerves, and both neuronal populations express opioid receptors [189]. When activated, opioid receptors decrease neuronal excitability and reduce neurotransmitter release. Neurons expressing opioid receptors in both the gut and the dorsal root ganglion (DRG) undergo homeostatic adaptations to chronic morphine that increase

baseline neuronal activity [190, 191]. This neuronal “superactivation” in response to chronic opioid manifests as tolerance in the presence of drug, and withdrawal signs, including hyperalgesia, upon removal of opioid [31]. Butyrate could change the course/severity of the homeostatic adaptations in neurons thought to underlie tolerance and/or hyperalgesia associated with chronic morphine administration (Figure 7). In support of a direct role of butyrate on neuronal excitability, co-administration of butyrate in morphine-treated mice prevents morphine-induced changes in excitability of opioid receptor expressing neurons in the DRG [47] thought to underlie hyperalgesia. In addition, as a ligand for two of its receptors, including the free-fatty acid receptor 3 (FFAR3) and GPR109A, which, like MOR, are Gi-coupled receptors, butyrate could mask either inflammatory-mediated or non-inflammatory mediated hyperexcitability by providing Gi signaling (Figure 7). These are not the only possibilities. For example, the microbiota has also been shown to alter brain levels of brain-derived neurotrophic factor (BDNF) independent of the vagus nerve [192], indicating the existence of microbial-produced signals that can cross the blood brain barrier beyond the DRG. SCFAs are one of several such microbial compounds known to be transmitted through the circulatory system that cross the blood-brain barrier [6, 193, 194]. The mice in our study underwent modest morphine treatment protocols that produced tolerance without significant hyperalgesia, and, as such, butyrate was protective for this tolerance even in the absence of hyperalgesia (Supplemental Figure 2; Supplemental Figure 13C,D). Hence, butyrate supplementation could be a useful tool for experimentally identifying and uncoupling parallel mechanisms that contribute to antinociceptive tolerance [47] (Figure 7, Supplemental Figure 14).

The most abundant biomarker of non-tolerance, *A. muciniphila*, was a particularly intriguing association due to its role in promoting gut homeostasis and barrier function through diverse mechanisms [12, 119, 182-185, 195, 196]. It is uniquely adapted to colonize the mucus layer and has a diverse enzyme repertoire to degrade and utilize mucin for growth [197]. It also liberates

nutrients from mucin to foster the growth of butyrate producers and its production of acetate enhances butyrate production by syntropy [110, 117, 198-201]. In part through its production of acetate, *A. muciniphila*, also stimulates mucin production and does so even better than *Lactobacillus plantarum*, one of the probiotic species previously shown to be protective against morphine dysbiosis and tolerance [202]. Even though pre-morphine microbiota composition was not predictive of non-tolerance, *A. muciniphila* was identified as one of the few biomarkers of non-tolerance prior to morphine (along with *Coprococcus*) and during mid-morphine (Figure 4B) when tolerant mice displayed microbiota instability (Figure 4C, Supplemental Figure 9). One could envision that the timing of its higher abundance could prime the mucosa and microbiota to resist some aspects of dysbiosis and did so better than native *Lactobacillus* and *Bifidobacterium,* which were elevated in tolerant mice pre-morphine (Figure 4B). In accordance with this, vancomycin pre-treatment, which substantially enriches for *A. muciniphila* [203, 204], curtails tolerance *in vivo* in mice and *in vitro* in neurons even without decreasing microbiota abundance- an affect suggested to be due to the concurrent general decrease in gram positive bacteria, many of which are mutualistic and produce butyrate [38, 106, 188]. Incidentally, vancomycin also improves aspects of autism spectrum disorder, a condition that correlates with low abundance of *A. muciniphila* [205], and with low SCFA production [206]. Combined, these suggest the possibility that *A. muciniphila* enhances the accumulation of neuroprotective compounds that curtail tolerance, rather than vancomycin simply eliminating gram positive bacteria and stemming inflammation. Many of the pathobionts identified here and in other studies are gram negative. The abundance of *A. muciniphila* increased in response to morphine, even modestly in mice that became tolerant, and as such it was not predictive for non-tolerance until post-morphine, where it was substantially depleted in tolerant mice (Figure 4B, Figure 5 and Table 2). As a mucin-degrading bacterium, one could foresee that a higher abundance at the wrong time, or in the absence of butyrate producers that support its immunomodulatory actions, could even compromise barrier functions under morphine stress [207]. This may explain why a probiotic

bacterium with so many potential benefits also positively correlates with some neurodegenerative disorders, underscoring the need for caution in employing live probiotics therapeutically while questions persist about modes of action and interaction among the complex microbiota [141, 208, 209].

In contrast with the convergence of microbiota and functions among non-tolerant mice, mice that became tolerant had fewer distinguishing microbiota signatures in common other than an increase in some pathobionts that were also predictive of tolerance (Figure 3, Figure 4B). What was apparent was a subtle difference in the timing of shared patterns of earlier disturbance, illustrated by changes in alpha diversity (Figure 4A), and emergence of taxa included in predictive models during early morphine compared to non-tolerant mice. The common microbiota signatures altered by morphine in tolerant mice include a number of recognized pathobionts linked to intestinal inflammation, including gram negative *Desulfovibrio* and *Bilophila,* and gram positive *Erysipelotrichaceae* and *Rhodococcus,* [210-220] as well as mucosa-associated taxa, even ones that produce butyrate, (e.g. *Anaerotruncus* and *Butyricicoccus;* [221]. The association of pathobionts with tolerance is compatible with the model that inappropriate pruning of mutualists, combined with a lack of adaptive responses trained on these rarer pathobionts, leads to overgrowth and uncontrolled inflammatory responses upon translocation (Supplemental Figure 14) [39, 41, 222-225]. Notably, mice that did not develop tolerance also had an increase in pathobiotic taxa and some were even predictive of non-tolerance at some phase of the paradigm (e.g. *Alphaproteobacteria RF32;* Figure 5*),* underscoring the importance of the temporality of dysbiosis that resulted from a loss of critical stabilizing community members as a contributing to differences in tolerance. The weaker resolution of microbiome associations with tolerance may reflect the fact that tolerant mice exhibited gradients in final antinociception: these mice were less alike than non-tolerant mice (Figure 5 and Supplemental Figure 11). If indeed there are multiple mechanisms of tolerance that

contribute to this variability, elucidating microbiome signatures for tolerance would be further constrained by our small cohort size (n=16 mice) where identification of signatures of non-tolerance benefitted from the higher statistical power of categorical assignment. Differentiation of mice that developed tolerance by different mechanisms would further be aided by assessment of additional morphine-driven behaviors that relate to OUD (e.g. mechanical antinociception, dependence, and impaired neuronal plasticity) [226, 227]. More comprehensive behavioral data would support the use of multivariate analyses [228] to extract meaningful signal in the microbiota of tolerant mice.

CONCLUSION

Opioids are critical tools in modern medicine and the mainstay for severe and post-operative pain treatment. Unfortunately, opioid use and the ensuing development of tolerance to the analgesic benefits without an accompanying development of tolerance to the respiratory suppressive effects of opioids increases the risk of overdose death as drug dose is necessarily increased to sustain pain management. Only a subset of humans, and as we show here mice, using opioids develop aspects of OUD yet there has been little mechanistic insight to explain this variability. In this study we demonstrate that the gut microbiota contributes to variability in the development of antinociceptive tolerance in a mouse model of OUD. Importantly, while we show that microbiota dysbiosis is an inevitable outcome of morphine use, tolerance is not, even in genetically inbred mice from the same vivarium. This emphasizes that, as with humans, mice used to model human disease conditions are not monolithic in part due to the flexible genome conferred by the microbiome. By capitalizing upon this variability, we could ascertain meaningful associations of the microbiota with variability in tolerance. We identify microbial biomarkers of protection from tolerance and show how functions provided by these microbes in the community, not individual microbes *per se,* underlie protection. We identified the function of butyrate production, and by proof-of-concept through dietetic supplementation, demonstrated

that it can reduce tolerance. Due to the foundational impact of germ theory of disease on the discipline of microbiology, microbes have been historically categorized as the problem, and this pervasive view has impeded progress in understanding the contributions of mutualistic community members to complex health conditions. Our study reinforces the importance of having a more holistic view to understand interactions between the microbiota and host. In the case of OUD, a better understanding of interactions among microbiota and between host and microbiota during morphine use could reveal underlying local or systemic mechanisms of tolerance, an understanding of which could reveal therapeutic targets and produce opportunities for effective pain management while limiting dangerous opioid side effects. Taken together, our studies indicate that the gut microbiota could be leveraged to reduce tolerance to the analgesic benefits of opioids and thereby reduced the risk of OUD.

ACKNOWLEDGMENTS

We thank Sarah W. Gooding, Madeline King, Joshua Gipoor, and Benjamin Wasson for assistance with data curation and collection; Maria Emanuel, Stephen Fiering, and Stephen Jones for their immeasurable support. We are grateful for the expertise of the staff at the Hubbard Center for Genome Studies at UNH and especially W. Kelley Thomas for advice, and Anthony Westbrook for bioinformatics assistance. We are grateful for the deep knowledge, helpful guidance, assistance and patience of Linnea Morley and Dean Elder at the Animal Resource Office at UNH.

DISCLOSURE STATEMENT

The authors have no competing interests to declare.

FUNDING DETAILS

This work was supported by the National Institutes of Drug Abuse under award numbers F31DA056222 (LF), R21DA049565 (JLW, CAW), R01DA055708 (JLW), and R15DA058187 (CAW, JLW); the National Institute of General Medical Sciences of the NIH through a New Hampshire- INBRE Institutional Development Award (IDeA), P20GM103506 (PI W. Green, award to CAW); the University of New Hampshire through a Collaborative Research Excellence pilot research partnerships project grant (CAW, JLW), a graduate school dissertation year fellowship and summer teaching assistant fellowship (IS), a research apprenticeship grant from the Hamel Center for Undergraduate Research (SM); the state of California as start-up funds (JLW).

DATA AVAILABILITY STATEMENT

The 16S amplicons that support the findings of this study are available in NCBI under the accession number PRJNA1098090. The authors confirm that all processed data supporting the findings of this study are available within the article and/or its supplementary materials.

REFERENCES

1. Carabotti M, Scirocco A, Maselli MA, Severi C. The gut-brain axis: interactions between enteric microbiota, central and enteric nervous systems. Ann Gastroenterol. 2015;28(2):203-9. PubMed PMID: 25830558; PMCID: PMC4367209.

2. Mayer EA. Gut feelings: the emerging biology of gut-brain communication. Nat Rev Neurosci. 2011;12(8):453-66. Epub 2011/07/14. doi: 10.1038/nrn3071. PubMed PMID: 21750565; PMCID: PMC3845678.

3. Cryan JF, Dinan TG. Mind-altering microorganisms: The impact of the gut microbiota on brain and behaviour. Nat Rev Neurosci. 2012;13(10):701-12. Epub 2012/09/13. doi: 10.1038/nrn3346. PubMed PMID: 22968153.

4. Cryan JF, O'Riordan KJ, Cowan CSM, Sandhu KV, Bastiaanssen TFS, Boehme M, Codagnone MG, Cussotto S, Fulling C, Golubeva AV, Guzzetta KE, Jaggar M, Long-Smith CM, Lyte JM, Martin JA, Molinero-Perez A, Moloney G, Morelli E, Morillas E, O'Connor R, Cruz-Pereira JS, Peterson VL, Rea K, Ritz NL, Sherwin E, Spichak S, Teichman EM, van de Wouw M, Ventura-Silva AP, Wallace-Fitzsimons SE, Hyland N, Clarke G, Dinan TG. The Microbiota-Gut-Brain Axis. Physiol Rev. 2019;99(4):1877-2013. doi: 10.1152/physrev.00018.2018. PubMed PMID: 31460832.

5. Griffiths JA, Mazmanian SK. Emerging evidence linking the gut microbiome to neurologic disorders. Genome Med. 2018;10(1):98. Epub 20181221. doi: 10.1186/s13073-018-0609-3. PubMed PMID: 30577867; PMCID: PMC6302417.

6. O'Riordan KJ, Collins MK, Moloney GM, Knox EG, Aburto MR, Fulling C, Morley SJ, Clarke G, Schellekens H, Cryan JF. Short chain fatty acids: Microbial metabolites for gut-brain axis signalling. Mol Cell Endocrinol. 2022;546:111572. Epub 20220120. doi: 10.1016/j.mce.2022.111572. PubMed PMID: 35066114.

7. Griffiths JA, Yoo BB, Thuy-Boun P, Cantu VJ, Weldon KC, Challis C, Sweredoski MJ, Chan KY, Thron TM, Sharon G, Moradian A, Humphrey G, Zhu Q, Shaffer JP, Wolan DW, Dorrestein PC, Knight R, Gradinaru V, Mazmanian SK. Peripheral neuronal activation shapes the microbiome and alters gut physiology. Cell Rep. 2024;43(4):113953. Epub 20240321. doi: 10.1016/j.celrep.2024.113953. PubMed PMID: 38517896.

8. Belkaid Y, Hand TW. Role of the microbiota in immunity and inflammation. Cell. 2014;157(1):121-41. doi: 10.1016/j.cell.2014.03.011. PubMed PMID: 24679531; PMCID: PMC4056765.

9. Goverse G, Molenaar R, Macia L, Tan J, Erkelens MN, Konijn T, Knippenberg M, Cook EC, Hanekamp D, Veldhoen M, Hartog A, Roeselers G, Mackay CR, Mebius RE. Diet-Derived Short Chain Fatty Acids Stimulate Intestinal Epithelial Cells To Induce Mucosal Tolerogenic Dendritic Cells. J Immunol. 2017;198(5):2172-81. Epub 20170118. doi: 10.4049/jimmunol.1600165. PubMed PMID: 28100682.

10. Schulthess J, Pandey S, Capitani M, Rue-Albrecht KC, Arnold I, Franchini F, Chomka A, Ilott NE, Johnston DGW, Pires E, McCullagh J, Sansom SN, Arancibia-Carcamo CV, Uhlig HH, Powrie F. The Short Chain Fatty Acid Butyrate Imprints an Antimicrobial Program in Macrophages. Immunity. 2019;50(2):432-45 e7. Epub 20190123. doi: 10.1016/j.immuni.2018.12.018. PubMed PMID: 30683619; PMCID: PMC6382411.

11. Silva YP, Bernardi A, Frozza RL. The Role of Short-Chain Fatty Acids From Gut Microbiota in Gut-Brain Communication. Front Endocrinol (Lausanne). 2020;11:25. Epub 20200131. doi: 10.3389/fendo.2020.00025. PubMed PMID: 32082260; PMCID: PMC7005631.

12. Cruz-Lebron A, Johnson R, Mazahery C, Troyer Z, Joussef-Pina S, Quinones-Mateu ME, Strauch CM, Hazen SL, Levine AD. Chronic opioid use modulates human enteric microbiota and intestinal barrier integrity. Gut microbes. 2021;13(1):1946368. doi: 10.1080/19490976.2021.1946368. PubMed PMID: 34313547; PMCID: PMC8317955.

13. Parada Venegas D, De la Fuente MK, Landskron G, González MJ, Quera R, Dijkstra G, Harmsen HJM, Faber KN, Hermoso MA. Short Chain Fatty Acids (SCFAs)-Mediated Gut Epithelial and Immune Regulation and Its Relevance for Inflammatory Bowel Diseases. Front Immunol. 2019;10:277. Epub 2019/03/28. doi: 10.3389/fimmu.2019.00277. PubMed PMID: 30915065; PMCID: PMC6421268.

14. Priyadarshini M, Kotlo KU, Dudeja PK, Layden BT. Role of Short Chain Fatty Acid Receptors in Intestinal Physiology and Pathophysiology. Compr Physiol. 2018;8(3):1091-115. Epub 20180618. doi: 10.1002/cphy.c170050. PubMed PMID: 29978895; PMCID: PMC6058973.

15. Koh A, De Vadder F, Kovatcheva-Datchary P, Backhed F. From Dietary Fiber to Host Physiology: Short-Chain Fatty Acids as Key Bacterial Metabolites. Cell. 2016;165(6):1332-45. doi: 10.1016/j.cell.2016.05.041. PubMed PMID: 27259147.

16. Haghikia A, Jorg S, Duscha A, Berg J, Manzel A, Waschbisch A, Hammer A, Lee DH, May C, Wilck N, Balogh A, Ostermann AI, Schebb NH, Akkad DA, Grohme DA, Kleinewietfeld M, Kempa S, Thone J, Demir S, Muller DN, Gold R, Linker RA. Dietary Fatty Acids Directly Impact Central Nervous System Autoimmunity via the Small Intestine. Immunity. 2015;43(4):817-29. doi: 10.1016/j.immuni.2015.09.007. PubMed PMID: 26488817.

17. Miller I. The gut-brain axis: Historical reflections. Microb Ecol Health Dis. 2018;29(1):1542921. Epub 2018/11/15. doi: 10.1080/16512235.2018.1542921. PubMed PMID: 30425612; PMCID: PMC6225396.

18. Rieder R, Wisniewski PJ, Alderman BL, Campbell SC. Microbes and mental health: A review. Brain Behav Immun. 2017;66:9-17. Epub 2017/01/31. doi: 10.1016/j.bbi.2017.01.016. PubMed PMID: 28131791.

19. Akbarali HI, Dewey WL. The gut-brain interaction in opioid tolerance. Curr Opin Pharmacol. 2017;37:126-30. Epub 20171113. doi: 10.1016/j.coph.2017.10.012. PubMed PMID: 29145012; PMCID: PMC5725258.

20. Kelly JR, Minuto C, Cryan JF, Clarke G, Dinan TG. Cross Talk: The Microbiota and Neurodevelopmental Disorders. Front Neurosci. 2017;11:490. Epub 2017/10/03. doi: 10.3389/fnins.2017.00490. PubMed PMID: 28966571; PMCID: PMC5605633.

21. Dinan TG, Cryan JF. Gut instincts: Microbiota as a key regulator of brain development, ageing and neurodegeneration. J Physiol. 2017;595(2):489-503. Epub 2016/09/20. doi: 10.1113/JP273106. PubMed PMID: 27641441; PMCID: PMC5233671.

22. Stefano GB, Pilonis N, Ptacek R, Raboch J, Vnukova M, Kream RM. Gut, microbiome, and brain regulatory axis: Relevance to neurodegenerative and psychiatric disorders. Cell Mol

Neurobiol. 2018;38(6):1197-206. Epub 2018/05/29. doi: 10.1007/s10571-018-0589-2. PubMed PMID: 29802603; PMCID: PMC6061125.

23. Farzi A, Hassan AM, Zenz G, Holzer P. Diabesity and mood disorders: Multiple links through the microbiota-gut-brain axis. Mol Aspects Med. 2018. Epub 2018/12/05. doi: 10.1016/j.mam.2018.11.003. PubMed PMID: 30513310.

24. Foster JA, Rinaman L, Cryan JF. Stress & the gut-brain axis: Regulation by the microbiome. Neurobiol Stress. 2017;7:124-36. Epub 2017/12/26. doi: 10.1016/j.ynstr.2017.03.001. PubMed PMID: 29276734; PMCID: PMC5736941.

25. Machelska H, Celik M. Opioid Receptors in Immune and Glial Cells-Implications for Pain Control. Front Immunol. 2020;11:300. Epub 20200304. doi: 10.3389/fimmu.2020.00300. PubMed PMID: 32194554; PMCID: PMC7064637.

26. Gooding SW, Whistler JL. A Balancing Act: Learning from the Past to Build a Future-Focused Opioid Strategy. Annu Rev Physiol. 2024;86:1-25. Epub 20231129. doi: 10.1146/annurev-physiol-042022-015914. PubMed PMID: 38029388; PMCID: PMC10987332.

27. Muchhala KH, Jacob JC, Kang M, Dewey WL, Akbarali HI. The Guts of the Opioid Crisis. Physiology (Bethesda). 2021;36(5):315-23. doi: 10.1152/physiol.00014.2021. PubMed PMID: 34431418; PMCID: PMC8813205.

28. Varrassi G, Fusco M, Skaper SD, Battelli D, Zis P, Coaccioli S, Pace MC, Paladini A. A Pharmacological Rationale to Reduce the Incidence of Opioid Induced Tolerance and Hyperalgesia: A Review. Pain Ther. 2018;7(1):59-75. Epub 20180328. doi: 10.1007/s40122-018-0094-9. PubMed PMID: 29594972; PMCID: PMC5993687.

29. Latremoliere A, Woolf CJ. Central sensitization: a generator of pain hypersensitivity by central neural plasticity. J Pain. 2009;10(9):895-926. doi: 10.1016/j.jpain.2009.06.012. PubMed PMID: 19712899; PMCID: PMC2750819.

30. Pergolizzi JV, Jr., Raffa RB, Rosenblatt MH. Opioid withdrawal symptoms, a consequence of chronic opioid use and opioid use disorder: Current understanding and

approaches to management. J Clin Pharm Ther. 2020;45(5):892-903. Epub 20200127. doi: 10.1111/jcpt.13114. PubMed PMID: 31986228.

31. Nestler EJ. Reflections on: "A general role for adaptations in G-Proteins and the cyclic AMP system in mediating the chronic actions of morphine and cocaine on neuronal function". Brain Res. 2016;1645:71-4. Epub 2016/01/08. doi: 10.1016/j.brainres.2015.12.039. PubMed PMID: 26740398; PMCID: 4927417.

32. Han B, Compton WM, Blanco C, Crane E, Lee J, Jones CM. Prescription Opioid Use, Misuse, and Use Disorders in U.S. Adults: 2015 National Survey on Drug Use and Health. Ann Intern Med. 2017;167(5):293-301. Epub 20170801. doi: 10.7326/M17-0865. PubMed PMID: 28761945.

33. Nadeau SE, Wu JK, Lawhern RA. Opioids and Chronic Pain: An Analytic Review of the Clinical Evidence. Front Pain Res (Lausanne). 2021;2:721357. Epub 20210817. doi: 10.3389/fpain.2021.721357. PubMed PMID: 35295493; PMCID: PMC8915556.

34. Volkow N, Benveniste H, McLellan AT. Use and Misuse of Opioids in Chronic Pain. Annu Rev Med. 2018;69:451-65. Epub 20171013. doi: 10.1146/annurev-med-011817-044739. PubMed PMID: 29029586.

35. Zhang L, Roy S. Opioid Modulation of the Gut-Brain Axis in Opioid-Associated Comorbidities. Cold Spring Harb Perspect Med. 2021;11(9). Epub 20210901. doi: 10.1101/cshperspect.a040485. PubMed PMID: 32816876; PMCID: PMC8415294.

36. Sobczak M, Salaga M, Storr MA, Fichna J. Physiology, signaling, and pharmacology of opioid receptors and their ligands in the gastrointestinal tract: Current concepts and future perspectives. J Gastroenterol. 2014;49(1):24-45. Epub 2013/02/12. doi: 10.1007/s00535-013-0753-x. PubMed PMID: 23397116; PMCID: PMC3895212.

37. Sikander A, Rana SV, Prasad KK. Role of serotonin in gastrointestinal motility and irritable bowel syndrome. Clin Chim Acta. 2009;403(1-2):47-55. Epub 20090204. doi: 10.1016/j.cca.2009.01.028. PubMed PMID: 19361459.

38. Kang M, Mischel RA, Bhave S, Komla E, Cho A, Huang C, Dewey WL, Akbarali HI. The effect of gut microbiome on tolerance to morphine mediated antinociception in mice. Scientific reports. 2017;7:42658. Epub 2017/02/18. doi: 10.1038/srep42658. PubMed PMID: 28211545; PMCID: PMC5314392.

39. Banerjee S, Sindberg G, Wang F, Meng J, Sharma U, Zhang L, Dauer P, Chen C, Dalluge J, Johnson T, Roy S. Opioid-induced gut microbial disruption and bile dysregulation leads to gut barrier compromise and sustained systemic inflammation. Mucosal Immunol. 2016;9(6):1418-28. Epub 2016/02/26. doi: 10.1038/mi.2016.9. PubMed PMID: 26906406; PMCID: PMC4996771.

40. Wang F, Meng J, Zhang L, Johnson T, Chen C, Roy S. Morphine induces changes in the gut microbiome and metabolome in a morphine dependence model. Scientific reports. 2018;8(1):3596. Epub 2018/02/28. doi: 10.1038/s41598-018-21915-8. PubMed PMID: 29483538; PMCID: PMC5827657.

41. Zhang L, Meng J, Ban Y, Jalodia R, Chupikova I, Fernandez I, Brito N, Sharma U, Abreu MT, Ramakrishnan S, Roy S. Morphine tolerance is attenuated in germfree mice and reversed by probiotics, implicating the role of gut microbiome. Proc Natl Acad Sci U S A. 2019;116(27):13523-32. Epub 20190617. doi: 10.1073/pnas.1901182116. PubMed PMID: 31209039; PMCID: PMC6613141.

42. Wang F, Roy S. Gut homeostasis, microbial dysbiosis, and opioids. Toxicol Pathol. 2017;45(1):150-6. Epub 20161128. doi: 10.1177/0192623316679898. PubMed PMID: 27895265; PMCID: PMC8607522.

43. Lee K, Vuong HE, Nusbaum DJ, Hsiao EY, Evans CJ, Taylor AMW. The gut microbiota mediates reward and sensory responses associated with regimen-selective morphine dependence. Neuropsychopharmacology. 2018;43(13):2606-14. Epub 2018/09/28. doi: 10.1038/s41386-018-0211-9. PubMed PMID: 30258112; PMCID: PMC6224506.

44. Hofford RS, Mervosh NL, Euston TJ, Meckel KR, Orr AT, Kiraly DD. Alterations in microbiome composition and metabolic byproducts drive behavioral and transcriptional responses to morphine. Neuropsychopharmacology. 2021;46(12):2062-72. Epub 2021/06/16. doi: 10.1038/s41386-021-01043-0. PubMed PMID: 34127799; PMCID: PMC8505488.

45. Simpson S, Kimbrough A, Boomhower B, McLellan R, Hughes M, Shankar K, de Guglielmo G, George O. Depletion of the microbiome alters the recruitment of neuronal ensembles of oxycodone intoxication and withdrawal. eNeuro. 2020;7(3). Epub 20200521. doi: 10.1523/ENEURO.0312-19.2020. PubMed PMID: 32341122; PMCID: PMC7242819.

46. Thomaz AC, Iyer V, Woodward TJ, Hohmann AG. Fecal microbiota transplantation and antibiotic treatment attenuate naloxone-precipitated opioid withdrawal in morphine-dependent mice. Exp Neurol. 2021;343:113787. Epub 20210618. doi: 10.1016/j.expneurol.2021.113787. PubMed PMID: 34153321; PMCID: PMC8477666.

47. Jessup D, Woods K, Thakker S, Damaj MI, Akbarali HI. Short-chain fatty acid, butyrate prevents morphine-and paclitaxel-induced nociceptive hypersensitivity. Scientific reports. 2023;13(1):17805. Epub 20231018. doi: 10.1038/s41598-023-44857-2. PubMed PMID: 37853033; PMCID: PMC10584825.

48. Komla E, Stevens DL, Zheng Y, Zhang Y, Dewey WL, Akbarali HI. Experimental Colitis Enhances the Rate of Antinociceptive Tolerance to Morphine via Peripheral Opioid Receptors. J Pharmacol Exp Ther. 2019;370(3):504-13. Epub 20190627. doi: 10.1124/jpet.119.256941. PubMed PMID: 31248978; PMCID: PMC6806632.

49. Gilbert JA, Quinn RA, Debelius J, Xu ZZ, Morton J, Garg N, Jansson JK, Dorrestein PC, Knight R. Microbiome-wide association studies link dynamic microbial consortia to disease. Nature. 2016;535(7610):94-103. Epub 2016/07/08. doi: 10.1038/nature18850. PubMed PMID: 27383984.

50. Brussow H. Problems with the concept of gut microbiota dysbiosis. Microb Biotechnol. 2020;13(2):423-34. Epub 20190826. doi: 10.1111/1751-7915.13479. PubMed PMID: 31448542; PMCID: PMC7017827.

51. Walker AW, Hoyles L. Human microbiome myths and misconceptions. Nat Microbiol. 2023;8(8):1392-6. Epub 20230731. doi: 10.1038/s41564-023-01426-7. PubMed PMID: 37524974.

52. Olesen SW, Alm EJ. Dysbiosis is not an answer. Nat Microbiol. 2016;1:16228. Epub 20161125. doi: 10.1038/nmicrobiol.2016.228. PubMed PMID: 27886190.

53. Felth L, Gooding S, Foxhall R, Rosa Z, Ireton K, Sall I, Gipoor J, Gaur A, King M, Dirks N, Whistler CA, Whistler JL. Deletion of arrestin-3 does not alter compulsive morphine-seeking behavior in an oral operant self-administration paradigm. bioRxiv. 2023:2023.03.30.534994. doi: 10.1101/2023.03.30.534994.

54. Wang J, Xu W, Wang R, Cheng R, Tang Z, Zhang M. The outer membrane protein Amuc_1100 of *Akkermansia muciniphila* promotes intestinal 5-HT biosynthesis and extracellular availability through TLR2 signalling. Food Funct. 2021;12(8):3597-610. doi: 10.1039/d1fo00115a. PubMed PMID: 33900345.

55. He L, Gooding SW, Lewis E, Felth LC, Gaur A, Whistler JL. Pharmacological and genetic manipulations at the micro-opioid receptor reveal arrestin-3 engagement limits analgesic tolerance and does not exacerbate respiratory depression in mice. Neuropsychopharmacology. 2021;46(13):2241-9. Epub 2021/07/15. doi: 10.1038/s41386-021-01054-x. PubMed PMID: 34257415; PMCID: PMC8581001.

56. Freedman D, Pisani, R., & Purves, R. Statistics (international student edition). Pisani RP, editor: WW Norton & Company, New York; 2007.

57. Kassambara A. ggpubr: 'ggplot2' Based Publication Ready Plots. R package version 0.6.0 2023. Available from: https://rpkgs.datanovia.com/ggpubr/.

58. Team RC. R: A Language and Environment for Statistical Computing. R Foundation for Statistical Computing, Vienna. 2013. Available from: http://www.R-project.org/.

59. Parada AE, Needham DM, Fuhrman JA. Every base matters: assessing small subunit rRNA primers for marine microbiomes with mock communities, time series and global field samples. Environ Microbiol. 2016;18(5):1403-14. Epub 20151014. doi: 10.1111/1462-2920.13023. PubMed PMID: 26271760.

60. Quince C, Lanzen A, Davenport RJ, Turnbaugh PJ. Removing noise from pyrosequenced amplicons. BMC Bioinformatics. 2011;12:38. Epub 20110128. doi: 10.1186/1471-2105-12-38. PubMed PMID: 21276213; PMCID: PMC3045300.

61. McMurdie PJ, Holmes S. phyloseq: an R package for reproducible interactive analysis and graphics of microbiome census data. PLoS One. 2013;8(4):e61217. Epub 20130422. doi: 10.1371/journal.pone.0061217. PubMed PMID: 23630581; PMCID: PMC3632530.

62. Martin M. Cutadapt removes adapter sequences from high-throughput sequencing reads. 2011. 2011;17(1):3. Epub 2011-08-02. doi: 10.14806/ej.17.1.200.

63. Bolyen E, Rideout JR, Dillon MR, Bokulich NA, Abnet CC, Al-Ghalith GA, Alexander H, Alm EJ, Arumugam M, Asnicar F, Bai Y, Bisanz JE, Bittinger K, Brejnrod A, Brislawn CJ, Brown CT, Callahan BJ, Caraballo-Rodriguez AM, Chase J, Cope EK, Da Silva R, Diener C, Dorrestein PC, Douglas GM, Durall DM, Duvallet C, Edwardson CF, Ernst M, Estaki M, Fouquier J, Gauglitz JM, Gibbons SM, Gibson DL, Gonzalez A, Gorlick K, Guo J, Hillmann B, Holmes S, Holste H, Huttenhower C, Huttley GA, Janssen S, Jarmusch AK, Jiang L, Kaehler BD, Kang KB, Keefe CR, Keim P, Kelley ST, Knights D, Koester I, Kosciolek T, Kreps J, Langille MGI, Lee J, Ley R, Liu YX, Loftfield E, Lozupone C, Maher M, Marotz C, Martin BD, McDonald D, McIver LJ, Melnik AV, Metcalf JL, Morgan SC, Morton JT, Naimey AT, Navas-Molina JA, Nothias LF, Orchanian SB, Pearson T, Peoples SL, Petras D, Preuss ML, Pruesse E, Rasmussen LB, Rivers A, Robeson MS, 2nd, Rosenthal P, Segata N, Shaffer M, Shiffer A, Sinha R, Song SJ, Spear JR, Swafford AD, Thompson LR, Torres PJ, Trinh P, Tripathi A, Turnbaugh PJ, Ul-Hasan

S, van der Hooft JJJ, Vargas F, Vazquez-Baeza Y, Vogtmann E, von Hippel M, Walters W, Wan Y, Wang M, Warren J, Weber KC, Williamson CHD, Willis AD, Xu ZZ, Zaneveld JR, Zhang Y, Zhu Q, Knight R, Caporaso JG. Reproducible, interactive, scalable and extensible microbiome data science using QIIME 2. Nat Biotechnol. 2019;37(8):852-7. doi: 10.1038/s41587-019-0209-9. PubMed PMID: 31341288; PMCID: PMC7015180.

64. Callahan BJ, Sankaran K, Fukuyama JA, McMurdie PJ, Holmes SP. Bioconductor Workflow for Microbiome Data Analysis: from raw reads to community analyses. F1000Res. 2016;5:1492. Epub 20160624. doi: 10.12688/f1000research.8986.2. PubMed PMID: 27508062; PMCID: PMC4955027.

65. McDonald D, Price MN, Goodrich J, Nawrocki EP, DeSantis TZ, Probst A, Andersen GL, Knight R, Hugenholtz P. An improved Greengenes taxonomy with explicit ranks for ecological and evolutionary analyses of bacteria and archaea. ISME J. 2012;6(3):610-8. Epub 2011/12/03. doi: 10.1038/ismej.2011.139. PubMed PMID: 22134646; PMCID: PMC3280142.

66. Camacho C, Coulouris G, Avagyan V, Ma N, Papadopoulos J, Bealer K, Madden TL. BLAST+: architecture and applications. BMC Bioinformatics. 2009;10:421. Epub 20091215. doi: 10.1186/1471-2105-10-421. PubMed PMID: 20003500; PMCID: PMC2803857.

67. Katoh K, Misawa K, Kuma K, Miyata T. MAFFT: a novel method for rapid multiple sequence alignment based on fast Fourier transform. Nucleic Acids Res. 2002;30(14):3059-66. doi: 10.1093/nar/gkf436. PubMed PMID: 12136088; PMCID: PMC135756.

68. Katoh K, Standley DM. MAFFT multiple sequence alignment software version 7: improvements in performance and usability. Mol Biol Evol. 2013;30(4):772-80. Epub 20130116. doi: 10.1093/molbev/mst010. PubMed PMID: 23329690; PMCID: PMC3603318.

69. Stamatakis A. RAxML-VI-HPC: maximum likelihood-based phylogenetic analyses with thousands of taxa and mixed models. Bioinformatics. 2006;22(21):2688-90. Epub 20060823. doi: 10.1093/bioinformatics/btl446. PubMed PMID: 16928733.

70. Leo Lahti SSea. Tools for microbiome analysis in R. Version Bioconductor2017. Available from: http://microbiome.github.com/microbiome.

71. Ma S, Shungin D, Mallick H, Schirmer M, Nguyen LH, Kolde R, Franzosa E, Vlamakis H, Xavier R, Huttenhower C. Population structure discovery in meta-analyzed microbial communities and inflammatory bowel disease using MMUPHin. Genome Biol. 2022;23(1):208. Epub 20221003. doi: 10.1186/s13059-022-02753-4. PubMed PMID: 36192803; PMCID: PMC9531436.

72. Lozupone CA, Hamady M, Kelley ST, Knight R. Quantitative and qualitative beta diversity measures lead to different insights into factors that structure microbial communities. Appl Environ Microbiol. 2007;73(5):1576-85. Epub 20070112. doi: 10.1128/AEM.01996-06. PubMed PMID: 17220268; PMCID: PMC1828774.

73. Lozupone C, Knight R. UniFrac: a new phylogenetic method for comparing microbial communities. Appl Environ Microbiol. 2005;71(12):8228-35. Epub 2005/12/08. doi: 10.1128/AEM.71.12.8228-8235.2005. PubMed PMID: 16332807; PMCID: PMC1317376.

74. Anderson MJ. Permutational Multivariate Analysis of Variance (PERMANOVA). Wiley StatsRef: Statistics Reference Online2014. p. 1-15.

75. Smith RJ. ecole: School of Ecology Package Unpublished R package in development2021.

76. Legendre PaL, L. Numerical Ecology. 3rd English ed. Elsevier., editor2012.

77. Legendre P, Oksanen J, ter Braak CJF. Testing the significance of canonical axes in redundancy analysis. Methods in Ecology and Evolution. 2011;2(3):269-77. doi: https://doi.org/10.1111/j.2041-210X.2010.00078.x.

78. Anderson MJ. Distance-based tests for homogeneity of multivariate dispersions2006.

79. O'Neill ME, Mathews KL. Levene tests of homogeneity of variance for general block and treatment designs. Biometrics. 2002;58(1):216-24. doi: 10.1111/j.0006-341x.2002.00216.x. PubMed PMID: 11890318.

80. Stier AC, Geange, S.W., Hanson, K.M., & Bolker, B.M. Predator density and timing of arrival affect reef fish community assembly2013.

81. Oksanen J SG, Blanchet F, Kindt R, Legendre P, Minchin P, O'Hara, R SP, Stevens M, Szoecs E, Wagner H, Barbour M, Bedward M, Bolker, B BD, Carvalho G, Chirico M, De Caceres M, Durand S, Evangelista, H FR, Friendly M, Furneaux B, Hannigan G, Hill M, Lahti L,, McGlinn D OM, Ribeiro Cunha E, Smith T, Stier A, Ter Braak C,, J W. _vegan: Community Ecology Package_. R package version

2.6-4, <https://CRAN.R-project.org/package=vegan>.2022.

82. Erdman C, Emerson JW. bcp: An R Package for Performing a Bayesian Analysis of Change Point Problems. Journal of Statistical Software. 2007;23(3):1 - 13. doi: 10.18637/jss.v023.i03.

83. Barry D, Hartigan JA. A Bayesian Analysis for Change Point Problems. Journal of the American Statistical Association. 1993;88(421):309-19. doi: 10.2307/2290726.

84. Martin BD, Witten D, Willis AD. Modeling microbial abundances and dysbiosis with beta-binomial regression. Ann Appl Stat. 2020;14(1):94-115. Epub 20200416. doi: 10.1214/19-aoas1283. PubMed PMID: 32983313; PMCID: PMC7514055.

85. Segata N, Izard J, Waldron L, Gevers D, Miropolsky L, Garrett WS, Huttenhower C. Metagenomic biomarker discovery and explanation. Genome Biol. 2011;12(6):R60. Epub 2011/06/28. doi: 10.1186/gb-2011-12-6-r60. PubMed PMID: 21702898; PMCID: PMC3218848.

86. De Caceres M, Legendre P. Associations between species and groups of sites: indices and statistical inference. Ecology. 2009;90(12):3566-74. doi: 10.1890/08-1823.1. PubMed PMID: 20120823.

87. Taylor LR, Woiwod IP, Perry JN. The Density-Dependence of Spatial Behaviour and the Rarity of Randomness. Journal of Animal Ecology. 1978;47(2):383-406. doi: 10.2307/3790.

88. Ma ZS. Power law analysis of the human microbiome. Mol Ecol. 2015;24(21):5428-45. doi: 10.1111/mec.13394. PubMed PMID: 26407082.

89. Marti JM. Robust Analysis of Time Series in Virome Metagenomics. Methods Mol Biol. 2018;1838:245-60. doi: 10.1007/978-1-4939-8682-8_17. PubMed PMID: 30129001.

90. Peschel S, Muller CL, von Mutius E, Boulesteix AL, Depner M. NetCoMi: network construction and comparison for microbiome data in R. Brief Bioinform. 2021;22(4). doi: 10.1093/bib/bbaa290. PubMed PMID: 33264391; PMCID: PMC8293835.

91. Douglas GM, Maffei VJ, Zaneveld JR, Yurgel SN, Brown JR, Taylor CM, Huttenhower C, Langille MGI. PICRUSt2 for prediction of metagenome functions. Nat Biotechnol. 2020;38(6):685-8. doi: 10.1038/s41587-020-0548-6. PubMed PMID: 32483366; PMCID: PMC7365738.

92. Louca S, Doebeli M. Efficient comparative phylogenetics on large trees. Bioinformatics. 2017;34(6):1053-5. doi: 10.1093/bioinformatics/btx701.

93. Barbera P, Kozlov AM, Czech L, Morel B, Darriba D, Flouri T, Stamatakis A. EPA-ng: Massively Parallel Evolutionary Placement of Genetic Sequences. Systematic Biology. 2018;68(2):365-9. doi: 10.1093/sysbio/syy054.

94. Czech L, Barbera P, Stamatakis A. Genesis and Gappa: processing, analyzing and visualizing phylogenetic (placement) data. Bioinformatics. 2020;36(10):3263-5. doi: 10.1093/bioinformatics/btaa070.

95. Mirarab S, Nguyen N, Warnow T. SEPP: SATé-enabled phylogenetic placement. Pac Symp Biocomput. 2012:247-58. doi: 10.1142/9789814366496_0024. PubMed PMID: 22174280.

96. Ye Y, Doak TG. A parsimony approach to biological pathway reconstruction/inference for genomes and metagenomes. PLoS Comput Biol. 2009;5(8):e1000465. Epub 20090814. doi: 10.1371/journal.pcbi.1000465. PubMed PMID: 19680427; PMCID: PMC2714467.

97. Yang C, Mai J, Cao X, Burberry A, Cominelli F, Zhang L. ggpicrust2: an R package for PICRUSt2 predicted functional profile analysis and visualization. Bioinformatics. 2023;39(8). doi: 10.1093/bioinformatics/btad470.

98. Rice TA, Bielecka AA, Nguyen MT, Rosen CE, Song D, Sonnert ND, Yang Y, Cao Y, Khetrapal V, Catanzaro JR, Martin AL, Rashed SA, Leopold SR, Hao L, Yu X, van Dijk D, Ring AM, Flavell RA, de Zoete MR, Palm NW. Interspecies commensal interactions have nonlinear impacts on host immunity. Cell Host Microbe. 2022;30(7):988-1002 e6. Epub 20220530. doi: 10.1016/j.chom.2022.05.004. PubMed PMID: 35640610; PMCID: PMC9283318.

99. Meng J, Yu H, Ma J, Wang J, Banerjee S, Charboneau R, Barke RA, Roy S. Morphine induces bacterial translocation in mice by compromising intestinal barrier function in a TLR-dependent manner. PLoS One. 2013;8(1):e54040. Epub 20130118. doi: 10.1371/journal.pone.0054040. PubMed PMID: 23349783; PMCID: PMC3548814.

100. Larsen JM. The immune response to *Prevotella* bacteria in chronic inflammatory disease. Immunology. 2017;151(4):363-74. Epub 20170620. doi: 10.1111/imm.12760. PubMed PMID: 28542929; PMCID: PMC5506432.

101. Kaakoush NO. Insights into the Role of Erysipelotrichaceae in the Human Host. Front Cell Infect Microbiol. 2015;5:84. Epub 20151120. doi: 10.3389/fcimb.2015.00084. PubMed PMID: 26636046; PMCID: PMC4653637.

102. Sayols-Baixeras S, Dekkers KF, Baldanzi G, Jonsson D, Hammar U, Lin YT, Ahmad S, Nguyen D, Varotsis G, Pita S, Nielsen N, Eklund AC, Holm JB, Nielsen HB, Ericson U, Brunkwall L, Ottosson F, Larsson A, Ericson D, Klinge B, Nilsson PM, Malinovschi A, Lind L, Bergstrom G, Sundstrom J, Arnlov J, Engstrom G, Smith JG, Orho-Melander M, Fall T. *Streptococcus* Species Abundance in the Gut Is Linked to Subclinical Coronary Atherosclerosis in 8973 Participants From the SCAPIS Cohort. Circulation. 2023;148(6):459-72. Epub 20230712. doi: 10.1161/CIRCULATIONAHA.123.063914. PubMed PMID: 37435755; PMCID: PMC10399955.

103. Tan J, Zhong Z, Tang Y, Qin W. Intestinal dysbiosis featuring abundance of Streptococcus associates with Henoch-Schonlein purpura nephritis (IgA vasculitis with nephritis) in adult. BMC Nephrol. 2022;23(1):10. Epub 20220103. doi: 10.1186/s12882-021-02638-x. PubMed PMID: 34979948; PMCID: PMC8722171.

104. Walsh CT, Levine RR. Studies of the enterohepatic circulation of morphine in the rat. J Pharmacol Exp Ther. 1975;195(2):303-10. Epub 1975/11/01. PubMed PMID: 1185599.

105. Lopetuso LR, Scaldaferri F, Petito V, Gasbarrini A. Commensal Clostridia: leading players in the maintenance of gut homeostasis. Gut Pathog. 2013;5(1):23. Epub 20130813. doi: 10.1186/1757-4749-5-23. PubMed PMID: 23941657; PMCID: PMC3751348.

106. Amiri P, Hosseini SA, Ghaffari S, Tutunchi H, Ghaffari S, Mosharkesh E, Asghari S, Roshanravan N. Role of Butyrate, a Gut Microbiota Derived Metabolite, in Cardiovascular Diseases: A comprehensive narrative review. Front Pharmacol. 2021;12:837509. Epub 20220202. doi: 10.3389/fphar.2021.837509. PubMed PMID: 35185553; PMCID: PMC8847574.

107. Riviere A, Selak M, Lantin D, Leroy F, De Vuyst L. Bifidobacteria and Butyrate-Producing Colon Bacteria: Importance and Strategies for Their Stimulation in the Human Gut. Front Microbiol. 2016;7:979. Epub 20160628. doi: 10.3389/fmicb.2016.00979. PubMed PMID: 27446020; PMCID: PMC4923077.

108. Chen W, Zhang S, Wu J, Ye T, Wang S, Wang P, Xing D. Butyrate-producing bacteria and the gut-heart axis in atherosclerosis. Clin Chim Acta. 2020;507:236-41. Epub 20200504. doi: 10.1016/j.cca.2020.04.037. PubMed PMID: 32376324.

109. Hiippala K, Barreto G, Burrello C, Diaz-Basabe A, Suutarinen M, Kainulainen V, Bowers JR, Lemmer D, Engelthaler DM, Eklund KK, Facciotti F, Satokari R. Novel *Odoribacter splanchnicus* strain and its outer membrane vesicles exert immunoregulatory cffects in vitro. Front Microbiol. 2020;11:575455. Epub 20201112. doi: 10.3389/fmicb.2020.575455. PubMed PMID: 33281770; PMCID: PMC7689251.

110. Xia J, Lv L, Liu B, Wang S, Zhang S, Wu Z, Yang L, Bian X, Wang Q, Wang K, Zhuge A, Li S, Yan R, Jiang H, Xu K, Li L. *Akkermansia muciniphila* ameliorates acetaminophen-Induced liver injury by regulating gut microbial composition and metabolism. Microbiol Spectr. 2022;10(1):e0159621. Epub 20220202. doi: 10.1128/spectrum.01596-21. PubMed PMID: 35107323; PMCID: PMC8809353.

111. Cui Y, Zhang L, Wang X, Yi Y, Shan Y, Liu B, Zhou Y, Lu X. Roles of intestinal Parabacteroides in human health and diseases. FEMS Microbiol Lett. 2022;369(1). doi: 10.1093/femsle/fnac072. PubMed PMID: 35945336.

112. Klaring K, Just S, Lagkouvardos I, Hanske L, Haller D, Blaut M, Wenning M, Clavel T. *Murimonas intestini* gen. nov., sp. nov., an acetate-producing bacterium of the family *Lachnospiraceae* isolated from the mouse gut. Int J Syst Evol Microbiol. 2015;65(Pt 3):870-8. Epub 20141217. doi: 10.1099/ijs.0.000030. PubMed PMID: 25519299.

113. Lai ZL, Tseng CH, Ho HJ, Cheung CKY, Lin JY, Chen YJ, Cheng FC, Hsu YC, Lin JT, El-Omar EM, Wu CY. Fecal microbiota transplantation confers beneficial metabolic effects of diet and exercise on diet-induced obese mice. Scientific reports. 2018;8(1):15625. Epub 2018/10/26. doi: 10.1038/s41598-018-33893-y. PubMed PMID: 30353027; PMCID: PMC6199268.

114. Taylor LR. Aggregation, Variance and the Mean. Nature. 1961;189(4766):732-5. doi: 10.1038/189732a0.

115. Taylor LR, Woiwod IP. Comparative Synoptic Dynamics. I. Relationships Between Inter- and Intra-Specific Spatial and Temporal Variance/Mean Population Parameters. Journal of Animal Ecology. 1982;51(3):879-906. doi: 10.2307/4012.

116. Kilpatrick AM, Ives AR. Species interactions can explain Taylor's power law for ecological time series. Nature. 2003;422(6927):65-8. doi: 10.1038/nature01471. PubMed PMID: 12621433.

117. Belzer C, Chia LW, Aalvink S, Chamlagain B, Piironen V, Knol J, de Vos WM. Microbial Metabolic Networks at the Mucus Layer Lead to Diet-Independent Butyrate and Vitamin B(12) Production by Intestinal Symbionts. mBio. 2017;8(5). Epub 20170919. doi: 10.1128/mBio.00770-17. PubMed PMID: 28928206; PMCID: PMC5605934.

118. Cani PD, de Vos WM. Next-Generation Beneficial Microbes: The case of *Akkermansia muciniphila*. Front Microbiol. 2017;8:1765. Epub 20170922. doi: 10.3389/fmicb.2017.01765. PubMed PMID: 29018410; PMCID: PMC5614963.

119. Depommier C, Everard A, Druart C, Plovier H, Van Hul M, Vieira-Silva S, Falony G, Raes J, Maiter D, Delzenne NM, de Barsy M, Loumaye A, Hermans MP, Thissen JP, de Vos WM, Cani PD. Supplementation with *Akkermansia muciniphila* in overweight and obese human volunteers: a proof-of-concept exploratory study. Nat Med. 2019;25(7):1096-103. Epub 20190701. doi: 10.1038/s41591-019-0495-2. PubMed PMID: 31263284; PMCID: PMC6699990.

120. Everard A, Belzer C, Geurts L, Ouwerkerk JP, Druart C, Bindels LB, Guiot Y, Derrien M, Muccioli GG, Delzenne NM, de Vos WM, Cani PD. Cross-talk between *Akkermansia muciniphila* and intestinal epithelium controls diet-induced obesity. Proc Natl Acad Sci U S A. 2013;110(22):9066-71. Epub 20130513. doi: 10.1073/pnas.1219451110. PubMed PMID: 23671105; PMCID: PMC3670398.

121. Si J, Kang H, You HJ, Ko G. Revisiting the role of *Akkermansia muciniphila* as a therapeutic bacterium. Gut microbes. 2022;14(1):2078619. doi: 10.1080/19490976.2022.2078619. PubMed PMID: 35613313.

122. Hou X, Zhang P, Du H, Chu W, Sun R, Qin S, Tian Y, Zhang Z, Xu F. *Akkermansia muciniphila* Potentiates the Antitumor Efficacy of FOLFOX in Colon Cancer. Front Pharmacol. 2021;12:725583. Epub 20210917. doi: 10.3389/fphar.2021.725583. PubMed PMID: 34603035; PMCID: PMC8484791.

123. Yang J, Li Y, Wen Z, Liu W, Meng L, Huang H. Oscillospira - a candidate for the next-generation probiotics. Gut microbes. 2021;13(1):1987783. doi: 10.1080/19490976.2021.1987783. PubMed PMID: 34693878; PMCID: PMC8547878.

124. Zhan S, Liu C, Meng J, Mao R, Tu T, Lin J, Chen M, Zeng Z, Zhuang X. Mucosa-Associated Oscillospira sp. Is Related to Intestinal Stricture and Post-Operative Disease Course in Crohn's Disease. Microorganisms. 2023;11(3). Epub 20230320. doi: 10.3390/microorganisms11030794. PubMed PMID: 36985367; PMCID: PMC10055919.

125. Parker BJ, Wearsch PA, Veloo ACM, Rodriguez-Palacios A. The Genus Alistipes: Gut Bacteria With Emerging Implications to Inflammation, Cancer, and Mental Health. Front Immunol. 2020;11:906. Epub 20200609. doi: 10.3389/fimmu.2020.00906. PubMed PMID: 32582143; PMCID: PMC7296073.

126. Caso JR, MacDowell KS, González-Pinto A, García S, de Diego-Adeliño J, Carceller-Sindreu M, Sarramea F, Caballero-Villarraso J, Gracia-García P, De la Cámara C, Agüera L, Gómez-Lus ML, Alba C, Rodríguez JM, Leza JC. Gut microbiota, innate immune pathways, and inflammatory control mechanisms in patients with major depressive disorder. Translational Psychiatry. 2021;11(1):645. doi: 10.1038/s41398-021-01755-3.

127. Shi J, Yang Y, Xu W, Cai H, Wu J, Long J, Cai Q, Zheng W, Flynn CR, Shu XO, Yu D. Sex-Specific Associations between Gut Microbiome and Non-Alcoholic Fatty Liver Disease among Urban Chinese Adults. Microorganisms. 2021;9(10). Epub 20211008. doi: 10.3390/microorganisms9102118. PubMed PMID: 34683439; PMCID: PMC8537656.

128. Yu D, Nguyen SM, Yang Y, Xu W, Cai H, Wu J, Cai Q, Long J, Zheng W, Shu XO. Long-term diet quality is associated with gut microbiome diversity and composition among urban Chinese adults. Am J Clin Nutr. 2021;113(3):684-94. doi: 10.1093/ajcn/nqaa350. PubMed PMID: 33471054; PMCID: PMC7948864.

129. Yang R, Shan S, Shi J, Li H, An N, Li S, Cui K, Guo H, Li Z. Coprococcus eutactus, a Potent Probiotic, Alleviates Colitis via Acetate-Mediated IgA Response and Microbiota

Restoration. J Agric Food Chem. 2023. Epub 20230214. doi: 10.1021/acs.jafc.2c06697. PubMed PMID: 36786768.

130. Vascellari S, Palmas V, Melis M, Pisanu S, Cusano R, Uva P, Perra D, Madau V, Sarchioto M, Oppo V, Simola N, Morelli M, Santoru ML, Atzori L, Melis M, Cossu G, Manzin A. Gut Microbiota and Metabolome Alterations Associated with Parkinson's Disease. mSystems. 2020;5(5). Epub 20200915. doi: 10.1128/mSystems.00561-20. PubMed PMID: 32934117; PMCID: PMC7498685.

131. Ju T, Kong JY, Stothard P, Willing BP. Defining the role of Parasutterella, a previously uncharacterized member of the core gut microbiota. ISME J. 2019;13(6):1520-34. Epub 20190211. doi: 10.1038/s41396-019-0364-5. PubMed PMID: 30742017; PMCID: PMC6776049.

132. Kolli U, Jalodia R, Moidunny S, Singh PK, Ban Y, Tao J, Cantu GN, Valdes E, Ramakrishnan S, Roy S. Multi-omics analysis revealing the interplay between gut microbiome and the host following opioid use. Gut microbes. 2023;15(2):2246184. doi: 10.1080/19490976.2023.2246184. PubMed PMID: 37610102; PMCID: PMC10448978.

133. Wlodarska M, Luo C, Kolde R, d'Hennezel E, Annand JW, Heim CE, Krastel P, Schmitt EK, Omar AS, Creasey EA, Garner AL, Mohammadi S, O'Connell DJ, Abubucker S, Arthur TD, Franzosa EA, Huttenhower C, Murphy LO, Haiser HJ, Vlamakis H, Porter JA, Xavier RJ. Indoleacrylic Acid Produced by Commensal Peptostreptococcus Species Suppresses Inflammation. Cell Host Microbe. 2017;22(1):25-37 e6. doi: 10.1016/j.chom.2017.06.007. PubMed PMID: 28704649; PMCID: PMC5672633.

134. Li X, Zhang B, Hu Y, Zhao Y. New Insights Into Gut-Bacteria-Derived Indole and Its Derivatives in Intestinal and Liver Diseases. Front Pharmacol. 2021;12:769501. Epub 20211213. doi: 10.3389/fphar.2021.769501. PubMed PMID: 34966278; PMCID: PMC8710772.

135. Knuesel T, Mohajeri MH. The Role of the Gut Microbiota in the Development and Progression of Major Depressive and Bipolar Disorder. Nutrients. 2022;14(1):37. PubMed PMID: doi:10.3390/nu14010037.

136. Chung YE, Chen HC, Chou HL, Chen IM, Lee MS, Chuang LC, Liu YW, Lu ML, Chen CH, Wu CS, Huang MC, Liao SC, Ni YH, Lai MS, Shih WL, Kuo PH. Exploration of microbiota targets for major depressive disorder and mood related traits. J Psychiatr Res. 2019;111:74-82. Epub 20190119. doi: 10.1016/j.jpsychires.2019.01.016. PubMed PMID: 30685565.

137. Vital M, Howe AC, Tiedje JM. Revealing the bacterial butyrate synthesis pathways by analyzing (meta)genomic data. mBio. 2014;5(2):e00889. Epub 20140422. doi: 10.1128/mBio.00889-14. PubMed PMID: 24757212; PMCID: PMC3994512.

138. Taylor AM, Thompson SV, Edwards CG, Musaad SMA, Khan NA, Holscher HD. Associations among diet, the gastrointestinal microbiota, and negative emotional states in adults. Nutr Neurosci. 2020;23(12):983-92. Epub 20190222. doi: 10.1080/1028415X.2019.1582578. PubMed PMID: 30794085.

139. Castro-Mejia J, Jakesevic M, Krych L, Nielsen DS, Hansen LH, Sondergaard BC, Kvist PH, Hansen AK, Holm TL. Treatment with a Monoclonal Anti-IL-12p40 Antibody Induces Substantial Gut Microbiota Changes in an Experimental Colitis Model. Gastroenterol Res Pract. 2016;2016:4953120. Epub 20160106. doi: 10.1155/2016/4953120. PubMed PMID: 26880890; PMCID: PMC4736578.

140. Zhou Q, Sun T, Wu F, Li F, Liu Y, Li W, Dai N, Tan L, Li T, Song Y. Correlation of gut microbiota and neurotransmitters in a rat model of post-traumatic stress disorder. Journal of Traditional Chinese Medical Sciences. 2020;7(4):375-85. doi: https://doi.org/10.1016/j.jtcms.2020.10.005.

141. Vacca M, Celano G, Calabrese FM, Portincasa P, Gobbetti M, De Angelis M. The Controversial Role of Human Gut Lachnospiraceae. Microorganisms. 2020;8(4). Epub 20200415. doi: 10.3390/microorganisms8040573. PubMed PMID: 32326636; PMCID: PMC7232163.

142. Tang D, Wang Y, Kang W, Zhou J, Dong R, Feng Q. Chitosan attenuates obesity by modifying the intestinal microbiota and increasing serum leptin levels in mice. Journal of Functional Foods. 2020;64:103659. doi: https://doi.org/10.1016/j.jff.2019.103659.

143. Liu X, Mao B, Gu J, Wu J, Cui S, Wang G, Zhao J, Zhang H, Chen W. Blautia-a new functional genus with potential probiotic properties? Gut microbes. 2021;13(1):1-21. doi: 10.1080/19490976.2021.1875796. PubMed PMID: 33525961; PMCID: PMC7872077.

144. Tavakkol Z, Samuelson D, deLancey Pulcini E, Underwood RA, Usui ML, Costerton JW, James GA, Olerud JE, Fleckman P. Resident bacterial flora in the skin of C57BL/6 mice housed under SPF conditions. J Am Assoc Lab Anim Sci. 2010;49(5):588-91. PubMed PMID: 20858360; PMCID: PMC2949428.

145. Yang L, Liu C, Zhao W, He C, Ding J, Dai R, Xu K, Xiao L, Luo L, Liu S, Li W, Meng H. Impaired Autophagy in Intestinal Epithelial Cells Alters Gut Microbiota and Host Immune Responses. Appl Environ Microbiol. 2018;84(18). Epub 20180831. doi: 10.1128/AEM.00880-18. PubMed PMID: 30006408; PMCID: PMC6121970.

146. Thompson CL, Mikaelyan A, Brune A. Immune-modulating gut symbionts are not "Candidatus Arthromitus". Mucosal Immunol. 2013;6(1):200-1. Epub 20120926. doi: 10.1038/mi.2012.91. PubMed PMID: 23013646.

147. Thompson CL, Vier R, Mikaelyan A, Wienemann T, Brune A. 'Candidatus Arthromitus' revised: segmented filamentous bacteria in arthropod guts are members of Lachnospiraceae. Environ Microbiol. 2012;14(6):1454-65. Epub 20120321. doi: 10.1111/j.1462-2920.2012.02731.x. PubMed PMID: 22436008.

148. Finegold SM, Lawson PA, Vaisanen ML, Molitoris DR, Song Y, Liu C, Collins MD. *Anaerofustis stercorihominis* gen. nov., sp. nov., from human feces. Anaerobe. 2004;10(1):41-5. doi: 10.1016/j.anaerobe.2003.10.002. PubMed PMID: 16701499.

149. Jakobsson HE, Rodriguez-Pineiro AM, Schutte A, Ermund A, Boysen P, Bemark M, Sommer F, Backhed F, Hansson GC, Johansson ME. The composition of the gut microbiota

shapes the colon mucus barrier. EMBO Rep. 2015;16(2):164-77. Epub 20141218. doi: 10.15252/embr.201439263. PubMed PMID: 25525071; PMCID: PMC4328744.

150. Kuehbacher T, Rehman A, Lepage P, Hellmig S, Folsch UR, Schreiber S, Ott SJ. Intestinal TM7 bacterial phylogenies in active inflammatory bowel disease. J Med Microbiol. 2008;57(Pt 12):1569-76. doi: 10.1099/jmm.0.47719-0. PubMed PMID: 19018031.

151. Inkster T, Wilson G, Black J, Mallon J, Connor M, Weinbren M. Cupriavidus spp. and other waterborne organisms in healthcare water systems across the UK. J Hosp Infect. 2022;123:80-6. Epub 20220216. doi: 10.1016/j.jhin.2022.02.003. PubMed PMID: 35181399.

152. Babrowski T, Holbrook C, Moss J, Gottlieb L, Valuckaite V, Zaborin A, Poroyko V, Liu DC, Zaborina O, Alverdy JC. Pseudomonas aeruginosa virulence expression is directly activated by morphine and is capable of causing lethal gut-derived sepsis in mice during chronic morphine administration. Ann Surg. 2012;255(2):386-93. doi: 10.1097/SLA.0b013e3182331870. PubMed PMID: 21989372; PMCID: PMC3258463.

153. Lankelma JM, Birnie E, Weehuizen TAF, Scicluna BP, Belzer C, Houtkooper RH, Roelofs J, de Vos AF, van der Poll T, Budding AE, Wiersinga WJ. The gut microbiota as a modulator of innate immunity during melioidosis. PLoS Negl Trop Dis. 2017;11(4):e0005548. Epub 20170419. doi: 10.1371/journal.pntd.0005548. PubMed PMID: 28422970; PMCID: PMC5411098.

154. Eberl L, Vandamme P. Members of the genus Burkholderia: good and bad guys. F1000Res. 2016;5. Epub 20160526. doi: 10.12688/f1000research.8221.1. PubMed PMID: 27303639; PMCID: PMC4882756.

155. Dean M, Cervellati C, Casanova E, Squerzanti M, Lanzara V, Medici A, Polverino De Laureto P, Bergamini CM. Characterization of cholylglycine hydrolase from a bile-adapted strain of Xanthomonas maltophilia and its application for quantitative hydrolysis of conjugated bile salts. Appl Environ Microbiol. 2002;68(6):3126-8. doi: 10.1128/AEM.68.6.3126-3128.2002. PubMed PMID: 12039776; PMCID: PMC123940.

156. Ndongo S, Beye M, Dubourg G, Nguyen TT, Couderc C, Fabrizio DP, Fournier PE, Raoult D, Angelakis E. Genome analysis and description of Xanthomonas massiliensis sp. nov., a new species isolated from human faeces. New Microbes New Infect. 2018;26:63-72. Epub 20180621. doi: 10.1016/j.nmni.2018.06.005. PubMed PMID: 30258635; PMCID: PMC6154774.

157. He Z, Zhao C, He Y, Liu Z, Fan G, Zhu K, Wang Y, Zhang N, Fu Y, Hu X. Enterogenic Stenotrophomonas maltophilia migrates to the mammary gland to induce mastitis by activating the calcium-ROS-AMPK-mTOR-autophagy pathway. J Anim Sci Biotechnol. 2023;14(1):157. Epub 20231220. doi: 10.1186/s40104-023-00952-y. PubMed PMID: 38124149; PMCID: PMC10731779.

158. Apisarnthanarak A, Fraser VJ, Dunne WM, Little JR, Hoppe-Bauer J, Mayfield JL, Polish LB. Stenotrophomonas maltophilia intestinal colonization in hospitalized oncology patients with diarrhea. Clin Infect Dis. 2003;37(8):1131-5. Epub 20030918. doi: 10.1086/378297. PubMed PMID: 14523780.

159. Hodgkinson K, El Abbar F, Dobranowski P, Manoogian J, Butcher J, Figeys D, Mack D, Stintzi A. Butyrate's role in human health and the current progress towards its clinical application to treat gastrointestinal disease. Clin Nutr. 2023;42(2):61-75. Epub 20221102. doi: 10.1016/j.clnu.2022.10.024. PubMed PMID: 36502573.

160. Chang PV, Hao L, Offermanns S, Medzhitov R. The microbial metabolite butyrate regulates intestinal macrophage function via histone deacetylase inhibition. Proc Natl Acad Sci U S A. 2014;111(6):2247-52. Epub 20140103. doi: 10.1073/pnas.1322269111. PubMed PMID: 24390544; PMCID: PMC3926023.

161. Singh V, Lee G, Son H, Koh H, Kim ES, Unno T, Shin JH. Butyrate producers, "The Sentinel of Gut": Their intestinal significance with and beyond butyrate, and prospective use as microbial therapeutics. Front Microbiol. 2022;13:1103836. Epub 20230112. doi: 10.3389/fmicb.2022.1103836. PubMed PMID: 36713166; PMCID: PMC9877435.

162. Simon JC, Marchesi JR, Mougel C, Selosse MA. Host-microbiota interactions: from holobiont theory to analysis. Microbiome. 2019;7(1):5. Epub 20190111. doi: 10.1186/s40168-019-0619-4. PubMed PMID: 30635058; PMCID: PMC6330386.

163. Nagpal J, Cryan JF. Host genetics, the microbiome & behaviour-a 'Holobiont' perspective. Cell Res. 2021;31(8):832-3. doi: 10.1038/s41422-021-00512-x. PubMed PMID: 33990786; PMCID: PMC8324890.

164. Buffington SA, Dooling SW, Sgritta M, Noecker C, Murillo OD, Felice DF, Turnbaugh PJ, Costa-Mattioli M. Dissecting the contribution of host genetics and the microbiome in complex behaviors. Cell. 2021;184(7):1740-56 e16. Epub 20210310. doi: 10.1016/j.cell.2021.02.009. PubMed PMID: 33705688; PMCID: PMC8996745.

165. Baganz NL, Blakely RD. A dialogue between the immune system and brain, spoken in the language of serotonin. ACS Chem Neurosci. 2013;4(1):48-63. Epub 20121207. doi: 10.1021/cn300186b. PubMed PMID: 23336044; PMCID: PMC3547518.

166. Thorburn AN, Macia L, Mackay CR. Diet, metabolites, and "western-lifestyle" inflammatory diseases. Immunity. 2014;40(6):833-42. doi: 10.1016/j.immuni.2014.05.014. PubMed PMID: 24950203.

167. Erny D, Hrabe de Angelis AL, Jaitin D, Wieghofer P, Staszewski O, David E, Keren-Shaul H, Mahlakoiv T, Jakobshagen K, Buch T, Schwierzeck V, Utermohlen O, Chun E, Garrett WS, McCoy KD, Diefenbach A, Staeheli P, Stecher B, Amit I, Prinz M. Host microbiota constantly control maturation and function of microglia in the CNS. Nat Neurosci. 2015;18(7):965-77. Epub 2015/06/02. doi: 10.1038/nn.4030. PubMed PMID: 26030851; PMCID: PMC5528863.

168. Dorrestein PC, Mazmanian SK, Knight R. Finding the missing links among metabolites, microbes, and the host. Immunity. 2014;40(6):824-32. doi: 10.1016/j.immuni.2014.05.015. PubMed PMID: 24950202; PMCID: PMC4503329.

169. Abu YF, Singh S, Tao J, Chupikova I, Singh P, Meng J, Roy S. Opioid-induced dysbiosis of maternal gut microbiota during gestation alters offspring gut microbiota and pain sensitivity. Gut microbes. 2024;16(1):2292224. Epub 20231218. doi: 10.1080/19490976.2023.2292224. PubMed PMID: 38108125; PMCID: PMC10730209.

170. Reichardt N, Vollmer M, Holtrop G, Farquharson FM, Wefers D, Bunzel M, Duncan SH, Drew JE, Williams LM, Milligan G, Preston T, Morrison D, Flint HJ, Louis P. Specific substrate-driven changes in human faecal microbiota composition contrast with functional redundancy in short-chain fatty acid production. ISME J. 2018;12(2):610-22. Epub 20171201. doi: 10.1038/ismej.2017.196. PubMed PMID: 29192904; PMCID: PMC5776475.

171. Hubbell SP. Neutral theory in community ecology and the hypothesis of functional equivalence2005.

172. Larsen OFA, Claassen E. The mechanistic link between health and gut microbiota diversity. Scientific reports. 2018;8(1):2183. Epub 20180201. doi: 10.1038/s41598-018-20141-6. PubMed PMID: 29391457; PMCID: PMC5794854.

173. Moya A, Ferrer M. Functional Redundancy-Induced Stability of Gut Microbiota Subjected to Disturbance. Trends Microbiol. 2016;24(5):402-13. Epub 20160317. doi: 10.1016/j.tim.2016.02.002. PubMed PMID: 26996765.

174. Furusawa Y, Obata Y, Fukuda S, Endo TA, Nakato G, Takahashi D, Nakanishi Y, Uetake C, Kato K, Kato T, Takahashi M, Fukuda NN, Murakami S, Miyauchi E, Hino S, Atarashi K, Onawa S, Fujimura Y, Lockett T, Clarke JM, Topping DL, Tomita M, Hori S, Ohara O, Morita T, Koseki H, Kikuchi J, Honda K, Hase K, Ohno H. Commensal microbe-derived butyrate induces the differentiation of colonic regulatory T cells. Nature. 2013;504(7480):446-50. Epub 20131113. doi: 10.1038/nature12721. PubMed PMID: 24226770.

175. Muchhala K, Kang M, Koseli E, Poklis J, Xu Q, Dewey W, Fettweis J, Jimenez N, Akbarali H. The Role of Morphine-Induced Impairment of Intestinal Epithelial Antibacterial Activity in Dysbiosis and its Impact on the Microbiota-Gut-Brain Axis. Res Sq. 2023. Epub

20230805. doi: 10.21203/rs.3.rs-3084467/v1. PubMed PMID: 37503065; PMCID: PMC10371156.

176. Hiippala K, Barreto G, Burrello C, Diaz-Basabe A, Suutarinen M, Kainulainen V, Bowers JR, Lemmer D, Engelthaler DM, Eklund KK, Facciotti F, Satokari R. Novel *Odoribacter splanchnicus* Strain and Its Outer Membrane Vesicles Exert Immunoregulatory Effects in vitro. Front Microbiol. 2020;11:575455. Epub 2020/12/08. doi: 10.3389/fmicb.2020.575455. PubMed PMID: 33281770; PMCID: PMC7689251.

177. Boesmans L, Valles-Colomer M, Wang J, Eeckhaut V, Falony G, Ducatelle R, Van Immerseel F, Raes J, Verbeke K. Butyrate Producers as Potential Next-Generation Probiotics: Safety Assessment of the Administration of Butyricicoccus pullicaecorum to Healthy Volunteers. mSystems. 2018;3(6). Epub 20181106. doi: 10.1128/mSystems.00094-18. PubMed PMID: 30417112; PMCID: PMC6222043.

178. Eeckhaut V, Machiels K, Perrier C, Romero C, Maes S, Flahou B, Steppe M, Haesebrouck F, Sas B, Ducatelle R, Vermeire S, Van Immerseel F. *Butyricicoccus pullicaecorum* in inflammatory bowel disease. Gut. 2013;62(12):1745-52. Epub 20121222. doi: 10.1136/gutjnl-2012-303611. PubMed PMID: 23263527.

179. Geirnaert A, Calatayud M, Grootaert C, Laukens D, Devriese S, Smagghe G, De Vos M, Boon N, Van de Wiele T. Butyrate-producing bacteria supplemented in vitro to Crohn's disease patient microbiota increased butyrate production and enhanced intestinal epithelial barrier integrity. Scientific reports. 2017;7(1):11450. Epub 20170913. doi: 10.1038/s41598-017-11734-8. PubMed PMID: 28904372; PMCID: PMC5597586.

180. Yang T, Ahmari N, Schmidt JT, Redler T, Arocha R, Pacholec K, Magee KL, Malphurs W, Owen JL, Krane GA, Li E, Wang GP, Vickroy TW, Raizada MK, Martyniuk CJ, Zubcevic J. Shifts in the Gut Microbiota Composition Due to Depleted Bone Marrow Beta Adrenergic Signaling Are Associated with Suppressed Inflammatory Transcriptional Networks in the Mouse

Colon. Front Physiol. 2017;8:220. Epub 20170412. doi: 10.3389/fphys.2017.00220. PubMed PMID: 28446880; PMCID: PMC5388758.

181. Devriese S, Eeckhaut V, Geirnaert A, Van den Bossche L, Hindryckx P, Van de Wiele T, Van Immerseel F, Ducatelle R, De Vos M, Laukens D. Reduced Mucosa-associated Butyricicoccus Activity in Patients with Ulcerative Colitis Correlates with Aberrant Claudin-1 Expression. J Crohns Colitis. 2017;11(2):229-36. Epub 20160801. doi: 10.1093/ecco-jcc/jjw142. PubMed PMID: 27484096.

182. Plovier H, Everard A, Druart C, Depommier C, Van Hul M, Geurts L, Chilloux J, Ottman N, Duparc T, Lichtenstein L, Myridakis A, Delzenne NM, Klievink J, Bhattacharjee A, van der Ark KC, Aalvink S, Martinez LO, Dumas ME, Maiter D, Loumaye A, Hermans MP, Thissen JP, Belzer C, de Vos WM, Cani PD. A purified membrane protein from *Akkermansia muciniphila* or the pasteurized bacterium improves metabolism in obese and diabetic mice. Nat Med. 2017;23(1):107-13. Epub 20161128. doi: 10.1038/nm.4236. PubMed PMID: 27892954.

183. Rao Y, Kuang Z, Li C, Guo S, Xu Y, Zhao D, Hu Y, Song B, Jiang Z, Ge Z, Liu X, Li C, Chen S, Ye J, Huang Z, Lu Y. Gut *Akkermansia muciniphila* ameliorates metabolic dysfunction-associated fatty liver disease by regulating the metabolism of L-aspartate via gut-liver axis. Gut microbes. 2021;13(1):1-19. doi: 10.1080/19490976.2021.1927633. PubMed PMID: 34030573; PMCID: PMC8158032.

184. Yoon HS, Cho CH, Yun MS, Jang SJ, You HJ, Kim JH, Han D, Cha KH, Moon SH, Lee K, Kim YJ, Lee SJ, Nam TW, Ko G. *Akkermansia muciniphila* secretes a glucagon-like peptide-1-inducing protein that improves glucose homeostasis and ameliorates metabolic disease in mice. Nat Microbiol. 2021;6(5):563-73. Epub 20210405. doi: 10.1038/s41564-021-00880-5. PubMed PMID: 33820962.

185. Yan J, Sheng L, Li H. *Akkermansia muciniphila*: is it the Holy Grail for ameliorating metabolic diseases? Gut microbes. 2021;13(1):1984104. doi: 10.1080/19490976.2021.1984104. PubMed PMID: 34674606; PMCID: PMC8726741.

186. Kim CH, Lee YU, Kim KH, Kang S, Kang GH, Chu H, Lee S. Comparison of Metabolites and Gut Microbes between Patients with Ulcerative Colitis and Healthy Individuals for an Integrative Medicine Approach to Ulcerative Colitis-A Pilot Observational Clinical Study (STROBE Compliant). Diagnostics (Basel). 2022;12(8). Epub 20220815. doi: 10.3390/diagnostics12081969. PubMed PMID: 36010319; PMCID: PMC9407185.

187. Bonnechere B, Amin N, van Duijn C. What Are the Key Gut Microbiota Involved in Neurological Diseases? A Systematic Review. Int J Mol Sci. 2022;23(22). Epub 20221108. doi: 10.3390/ijms232213665. PubMed PMID: 36430144; PMCID: PMC9696257.

188. Mischel RA, Muchhala KH, Dewey WL, Akbarali HI. The "Culture" of Pain Control: A Review of Opioid-Induced Dysbiosis (OID) in Antinociceptive Tolerance. J Pain. 2020;21(7-8):751-62. Epub 20191211. doi: 10.1016/j.jpain.2019.11.015. PubMed PMID: 31841668; PMCID: PMC7286790.

189. Stein C. Opioid Receptors. Annu Rev Med. 2016;67:433-51. Epub 20150826. doi: 10.1146/annurev-med-062613-093100. PubMed PMID: 26332001.

190. Ossipov MH, Lai J, King T, Vanderah TW, Porreca F. Underlying mechanisms of pronociceptive consequences of prolonged morphine exposure. Biopolymers. 2005;80(2-3):319-24. doi: 10.1002/bip.20254. PubMed PMID: 15795927.

191. Akbarali HI, Inkisar A, Dewey WL. Site and mechanism of morphine tolerance in the gastrointestinal tract. Neurogastroenterol Motil. 2014;26(10):1361-7. doi: 10.1111/nmo.12443. PubMed PMID: 25257923; PMCID: PMC4423201.

192. Bercik P, Denou E, Collins J, Jackson W, Lu J, Jury J, Deng Y, Blennerhassett P, Macri J, McCoy KD, Verdu EF, Collins SM. The intestinal microbiota affect central levels of brain-derived neurotropic factor and behavior in mice. Gastroenterology. 2011;141(2):599-609, e1-3. Epub 20110430. doi: 10.1053/j.gastro.2011.04.052. PubMed PMID: 21683077.

193. Hoyles L, Pontifex MG, Rodriguez-Ramiro I, Anis-Alavi MA, Jelane KS, Snelling T, Solito E, Fonseca S, Carvalho AL, Carding SR, Muller M, Glen RC, Vauzour D, McArthur S.

Regulation of blood-brain barrier integrity by microbiome-associated methylamines and cognition by trimethylamine N-oxide. Microbiome. 2021;9(1):235. Epub 20211127. doi: 10.1186/s40168-021-01181-z. PubMed PMID: 34836554; PMCID: PMC8626999.

194. Margolis KG, Cryan JF, Mayer EA. The Microbiota-Gut-Brain Axis: From Motility to Mood. Gastroenterology. 2021;160(5):1486-501. Epub 20210122. doi: 10.1053/j.gastro.2020.10.066. PubMed PMID: 33493503; PMCID: PMC8634751.

195. Reunanen J, Kainulainen V, Huuskonen L, Ottman N, Belzer C, Huhtinen H, de Vos WM, Satokari R. *Akkermansia muciniphila* Adheres to Enterocytes and Strengthens the Integrity of the Epithelial Cell Layer. Appl Environ Microbiol. 2015;81(11):3655-62. Epub 20150320. doi: 10.1128/AEM.04050-14. PubMed PMID: 25795669; PMCID: PMC4421065.

196. Chelakkot C, Choi Y, Kim DK, Park HT, Ghim J, Kwon Y, Jeon J, Kim MS, Jee YK, Gho YS, Park HS, Kim YK, Ryu SH. *Akkermansia muciniphila*-derived extracellular vesicles influence gut permeability through the regulation of tight junctions. Exp Mol Med. 2018;50(2):e450. Epub 20180223. doi: 10.1038/emm.2017.282. PubMed PMID: 29472701; PMCID: PMC5903829.

197. Derrien M, Vaughan EE, Plugge CM, de Vos WM. *Akkermansia muciniphila* gen. nov., sp. nov., a human intestinal mucin-degrading bacterium. Int J Syst Evol Microbiol. 2004;54(Pt 5):1469-76. doi: 10.1099/ijs.0.02873-0. PubMed PMID: 15388697.

198. van Passel MW, Kant R, Zoetendal EG, Plugge CM, Derrien M, Malfatti SA, Chain PS, Woyke T, Palva A, de Vos WM, Smidt H. The genome of

, a dedicated intestinal mucin degrader, and its use in exploring intestinal metagenomes. PLoS One. 2011;6(3):e16876. Epub 2011/03/11. doi: 10.1371/journal.pone.0016876. PubMed PMID: 21390229; PMCID: PMC3048395.

199. Liu L, Huh JR, Shah K. Microbiota and the gut-brain-axis: Implications for new therapeutic design in the CNS. EBioMedicine. 2022;77:103908. Epub 20220304. doi: 10.1016/j.ebiom.2022.103908. PubMed PMID: 35255456; PMCID: PMC8897630.

200. Sun X, Cui Q, Ni J, Liu X, Zhu J, Zhou T, Huang H, OuYang K, Wu Y, Yang Z. Retracted and Republished from: "Gut Microbiota Mediates the Therapeutic Effect of Monoclonal Anti-TLR4 Antibody on Acetaminophen-Induced Acute Liver Injury in Mice". Microbiol Spectr. 2023;11(2):e0471522. Epub 20230321. doi: 10.1128/spectrum.04715-22. PubMed PMID: 36942972; PMCID: PMC10186863.

201. Zou H, Zhang M, Zhu X, Zhu L, Chen S, Luo M, Xie Q, Chen Y, Zhang K, Bu Q, Wei Y, Ye T, Li Q, Yan X, Zhou Z, Yang C, Li Y, Zhou H, Zhang C, You X, Zheng G, Zhao G. Ginsenoside Rb1 improves metabolic disorder in high-fat diet-induced obese mice associated with modulation of gut microbiota. Front Microbiol. 2022;13:826487. Epub 20220419. doi: 10.3389/fmicb.2022.826487. PubMed PMID: 35516426; PMCID: PMC9062662.

202. van der Lugt B, van Beek AA, Aalvink S, Meijer B, Sovran B, Vermeij WP, Brandt RMC, de Vos WM, Savelkoul HFJ, Steegenga WT, Belzer C. *Akkermansia muciniphila* ameliorates the age-related decline in colonic mucus thickness and attenuates immune activation in accelerated aging Ercc1 (-/Delta7) mice. Immun Ageing. 2019;16:6. Epub 20190308. doi: 10.1186/s12979-019-0145-z. PubMed PMID: 30899315; PMCID: PMC6408808.

203. Hansen CH, Krych L, Nielsen DS, Vogensen FK, Hansen LH, Sorensen SJ, Buschard K, Hansen AK. Early life treatment with vancomycin propagates *Akkermansia muciniphila* and reduces diabetes incidence in the NOD mouse. Diabetologia. 2012;55(8):2285-94. Epub 20120510. doi: 10.1007/s00125-012-2564-7. PubMed PMID: 22572803.

204. Ousey J, Boktor JC, Mazmanian SK. Gut microbiota suppress feeding induced by palatable foods. Curr Biol. 2023;33(1):147-57 e7. Epub 20221129. doi: 10.1016/j.cub.2022.10.066. PubMed PMID: 36450285; PMCID: PMC9839363.

205. Sandler RH, Finegold SM, Bolte ER, Buchanan CP, Maxwell AP, Vaisanen ML, Nelson MN, Wexler HM. Short-term benefit from oral vancomycin treatment of regressive-onset autism. J Child Neurol. 2000;15(7):429-35. doi: 10.1177/088307380001500701. PubMed PMID: 10921511.

206. Adams JB, Johansen LJ, Powell LD, Quig D, Rubin RA. Gastrointestinal flora and gastrointestinal status in children with autism--comparisons to typical children and correlation with autism severity. BMC Gastroenterol. 2011;11:22. Epub 20110316. doi: 10.1186/1471-230x-11-22. PubMed PMID: 21410934; PMCID: PMC3072352.

207. Qu S, Zheng Y, Huang Y, Feng Y, Xu K, Zhang W, Wang Y, Nie K, Qin M. Excessive consumption of mucin by over-colonized *Akkermansia muciniphila* promotes intestinal barrier damage during malignant intestinal environment. Front Microbiol. 2023;14:1111911. Epub 20230302. doi: 10.3389/fmicb.2023.1111911. PubMed PMID: 36937258; PMCID: PMC10018180.

208. Chiantera V, Lagana AS, Basciani S, Nordio M, Bizzarri M. A Critical Perspective on the Supplementation of Akkermansia muciniphila: Benefits and Harms. Life (Basel). 2023;13(6). Epub 20230524. doi: 10.3390/life13061247. PubMed PMID: 37374030; PMCID: PMC10301191.

209. Wang K, Wu W, Wang Q, Yang L, Bian X, Jiang X, Lv L, Yan R, Xia J, Han S, Li L. The negative effect of

-mediated post-antibiotic reconstitution of the gut microbiota on the development of colitis-associated colorectal cancer in mice. Front Microbiol. 2022;13:932047. Epub 20221014. doi: 10.3389/fmicb.2022.932047. PubMed PMID: 36312913; PMCID: PMC9614165.

210. Singh SB, Carroll-Portillo A, Lin HC. Desulfovibrio in the Gut: The Enemy within? Microorganisms. 2023;11(7). Epub 20230707. doi: 10.3390/microorganisms11071772. PubMed PMID: 37512944; PMCID: PMC10383351.

211. Murros KE, Huynh VA, Takala TM, Saris PEJ. *Desulfovibrio* bacteria are associated with Parkinson's Disease. Front Cell Infect Microbiol. 2021;11:652617. Epub 20210503. doi: 10.3389/fcimb.2021.652617. PubMed PMID: 34012926; PMCID: PMC8126658.

212. Sampson TR, Debelius JW, Thron T, Janssen S, Shastri GG, Ilhan ZE, Challis C, Schretter CE, Rocha S, Gradinaru V, Chesselet MF, Keshavarzian A, Shannon KM, Krajmalnik-

Brown R, Wittung-Stafshede P, Knight R, Mazmanian SK. Gut microbiota regulate motor deficits and neuroinflammation in a model of Parkinson's disease. Cell. 2016;167(6):1469-80 e12. Epub 2016/12/03. doi: 10.1016/j.cell.2016.11.018. PubMed PMID: 27912057; PMCID: PMC5718049.

213. Caputi V, Giron MC. Microbiome-gut-brain axis and toll-Like receptors in Parkinson's disease. Int J Mol Sci. 2018;19(6). Epub 2018/06/09. doi: 10.3390/ijms19061689. PubMed PMID: 29882798; PMCID: PMC6032048.

214. Forbes JD, Van Domselaar G, Bernstein CN. The Gut Microbiota in Immune-Mediated Inflammatory Diseases. Front Microbiol. 2016;7:1081. Epub 20160711. doi: 10.3389/fmicb.2016.01081. PubMed PMID: 27462309; PMCID: PMC4939298.

215. Guerrero C, Tort J, Perez J, Andres M, Espejo E. *Rhodococcus equi* infection in a patient with Crohn's disease treated with infliximab. J Infect. 2015;70(6):689-90. Epub 20141227. doi: 10.1016/j.jinf.2014.12.008. PubMed PMID: 25546345.

216. Darrah PA, Monaco MC, Jain S, Hondalus MK, Golenbock DT, Mosser DM. Innate immune responses to *Rhodococcus equi*. J Immunol. 2004;173(3):1914-24. doi: 10.4049/jimmunol.173.3.1914. PubMed PMID: 15265925.

217. Lin X, Abdalla M, Yang J, Liu L, Fu Y, Zhang Y, Yang S, Yu H, Ge Y, Zhang S, Kang G, Dang W, Jiang Q, Wang Y, Gai Z. Relationship between gut microbiota dysbiosis and immune indicator in children with sepsis. BMC Pediatr. 2023;23(1):516. Epub 20231016. doi: 10.1186/s12887-023-04349-8. PubMed PMID: 37845615; PMCID: PMC10578006.

218. Berry D, Reinisch W. Intestinal microbiota: a source of novel biomarkers in inflammatory bowel diseases? Best Pract Res Clin Gastroenterol. 2013;27(1):47-58. doi: 10.1016/j.bpg.2013.03.005. PubMed PMID: 23768552.

219. Feng Z, Long W, Hao B, Ding D, Ma X, Zhao L, Pang X. A human stool-derived *Bilophila wadsworthia* strain caused systemic inflammation in specific-pathogen-free mice. Gut Pathog. 2017;9:59. Epub 20171026. doi: 10.1186/s13099-017-0208-7. PubMed PMID: 29090023; PMCID: PMC5657053.

220. Turnbaugh PJ. Microbiology: fat, bile and gut microbes. Nature. 2012;487(7405):47-8. Epub 20120704. doi: 10.1038/487047a. PubMed PMID: 22763552.

221. Comelli EM, Simmering R, Faure M, Donnicola D, Mansourian R, Rochat F, Corthesy-Theulaz I, Cherbut C. Multifaceted transcriptional regulation of the murine intestinal mucus layer by endogenous microbiota. Genomics. 2008;91(1):70-7. Epub 20071126. doi: 10.1016/j.ygeno.2007.09.006. PubMed PMID: 18035521.

222. Jacobs JP, Braun J. Immune and genetic gardening of the intestinal microbiome. FEBS letters. 2014;588(22):4102-11. Epub 20140305. doi: 10.1016/j.febslet.2014.02.052. PubMed PMID: 24613921; PMCID: PMC4156569.

223. Zhu B, Wang X, Li L. Human gut microbiome: the second genome of human body. Protein Cell. 2010;1(8):718-25. Epub 20100828. doi: 10.1007/s13238-010-0093-z. PubMed PMID: 21203913; PMCID: PMC4875195.

224. Begum N, Mandhare A, Tryphena KP, Srivastava S, Shaikh MF, Singh SB, Khatri DK. Epigenetics in depression and gut-brain axis: A molecular crosstalk. Front Aging Neurosci. 2022;14:1048333. Epub 20221213. doi: 10.3389/fnagi.2022.1048333. PubMed PMID: 36583185; PMCID: PMC9794020.

225. van Zyl WF, Deane SM, Dicks LMT. Molecular insights into probiotic mechanisms of action employed against intestinal pathogenic bacteria. Gut microbes. 2020;12(1):1831339. doi: 10.1080/19490976.2020.1831339. PubMed PMID: 33112695; PMCID: PMC7595611.

226. Treadway MT, Cooper JA, Miller AH. Can't or Won't? Immunometabolic Constraints on Dopaminergic Drive. Trends Cogn Sci. 2019;23(5):435-48. Epub 2019/04/06. doi: 10.1016/j.tics.2019.03.003. PubMed PMID: 30948204; PMCID: PMC6839942.

227. Paul AK, Smith CM, Rahmatullah M, Nissapatorn V, Wilairatana P, Spetea M, Gueven N, Dietis N. Opioid Analgesia and Opioid-Induced Adverse Effects: A Review. Pharmaceuticals (Basel). 2021;14(11). Epub 20211027. doi: 10.3390/ph14111091. PubMed PMID: 34832873; PMCID: PMC8620360.

228. Mallick H, Rahnavard A, McIver LJ, Ma S, Zhang Y, Nguyen LH, Tickle TL, Weingart G, Ren B, Schwager EH, Chatterjee S, Thompson KN, Wilkinson JE, Subramanian A, Lu Y, Waldron L, Paulson JN, Franzosa EA, Bravo HC, Huttenhower C. Multivariable association discovery in population-scale meta-omics studies. PLoS Comput Biol. 2021;17(11):e1009442. Epub 20211116. doi: 10.1371/journal.pcbi.1009442. PubMed PMID: 34784344; PMCID: PMC8714082.

Table 1: Indicator taxa of morphine tolerant and non-tolerant microbiota.

Morphine	Development of Tolerance	Community Member	Specificity[1] Probability	Sensitivity[2] Probability	Indicator[3] Value	p-value
Pre	No	*Rikenellaceae AF12* (ASV_344)[4]	0.7955	0.1944	0.393	0.038
Early	No	*Burkholderia* (ASV_1302)[5]	0.8929	0.2778	0.498	0.024
	No	*Xanthomonas* (ASV_2124)[5]	1	0.1667	0.408	0.045
Mid	No	*Parabacteroides* (ASV_66)[5]	0.7852	0.375	0.543	0.012
Late	No	*RF32* (ASV_474) [5]	0.7353	0.5556	0.639	0.001
	No	*AF12* (ASV_344)[4]	0.8475	0.2778	0.485	0.004
	No	*F16* (ASV_1026) [5]	0.7534	0.3056	0.48	0.018
	Yes	*Rhodococcus* (ASV_1977)[5]	1	0.15	0.387	0.021
Post	No	*Anaerofustis* (ASV_779)[5]	0.7143	0.7143	0.714	0.001
	No	*Odoribacter* (ASV_189)[4]	0.6829	0.5714	0.625	0.008
	No	*RF32* (ASV_474)[5]	0.7538	0.5	0.614	0.005
	No	*F16* (ASV_1026)[5]	0.7333	0.3929	0.537	0.015
	No	*Stenotrophomonas*[5] (ASV_7876)	1	0.1071	0.327	0.047
	Yes	*Streptococcus* (ASV_869)[5]	1	0.2245	0.474	0.02
All	No	*RF32* (ASV_474)[5]	0.70664	0.31081	0.469	0.001
	No	*AF12* (ASV_344)[4]	0.73464	0.25676	0.434	0.001
	No	*F16* (ASV_1026)[5]	0.71212	0.20946	0.386	0.002
	No	*Flexispira* (ASV_704)[4]	1	0.02027	0.142	0.038
	Yes	*Bilophila* (ASV_791) [5, 6]	0.7886	0.1008	0.282	0.016

[1] Specificity is the estimate of the probability that the ASV belongs to the experience given the fact that the ASV was found. This conditional probability is called the *specificity* or *positive predictive value* of the species as indicator of the site group

[2] Sensitivity is sample estimate of the probability of finding the ASV in samples belonging to the experience. This second conditional probability is called the *fidelity* or *sensitivity* of the ASV as indicator of the target site group

[3] Indicator value index (accounts for unequal group sizes) given probabilities A and B

[4] Identified as a biomarker of non-tolerance but not influenced by morphine use (See Figure 4)

[5] Identified as biomarker, indicator species, or by centrality measures and linked to morphine use (See Figure 3A and Supplemental Table 3)

[6] Identified in higher abundance in mice with poor starting antinociception (see Supplemental Figure 8)

1697 **Table 2: Notable features of microbiota associated with non-tolerant mice[1]**

Taxa	Association[2]	Experience	Notable Feature(s)
Akkermansia muciniphila (ASV_2)[3]	B A M	Pre, Mid Early, Late Post	Mucin degrading, acetate producer; syntrophic support of **butyrate** producers[107, 117] Modulates immune responses and gut homeostasis [118-122]
Oscillospira (Oscillibacter ruminatium) (ASV_38)[3]	B A	Late, Post Early-Late/Post	**Butyrate** [123] Chronic constipation correlated with CD post-operative remission [123, 124]
Rikenellaceae (Alistipes onderdonkii) (ASV_22)	M	Mid	Potential acetate and propionate producer based on taxa [125] May affect tryptophan bioavailability in MDD [126]
Mollicutes RF39 *(Breznakia pachnodae)*(ASV_28)[3]	B	Late	Acetate producer; inversely correlated with inflammation, and BMI [127, 128]
Coprococcus (*Eubacterium xylanophilum*) (ASV_96)[3]	B	Pre-	**Butyrate** and acetate based on taxa; inversely correlates with IBD, depression and PD [106, 129, 130]
Sutterella (*Parasutterella excrementihominis*) (ASV_76)	B	Late, Post	Bile acid maintenance [131] Morphine dysbiosis, inflammation [132]
Peptostreptococcaceae (Romboutsia timonensis) (ASV_72)	M	Mid, Post	Mucin degrading, tryptophan metabolism and indole acrylic acid production promotes barrier function; controversially (positively/negatively) correlated with anxiety and depressive disorders [133-136]
Parabacteroides (Parabacteroides chongii) (ASV_66)	I M	Early-Mid Mid, All	**Butyrate**, anti-inflammatory [111]
Odoribacter (Odoribacter splanchnicus) (ASV_189)	B A I	Combined Pre-Late/Post Early, Late, Post	**Butyrate**, inversely correlated with gut inflammation, associated with exercise and weight control [110, 113, 137, 138, 176]
Erysipelotrichaceae (Clostridum; *Longibaculum muris*) (ASV_143)[3]	B	Late, Post	Glucose absorption/glycemic control; Linked to intestinal inflammation [101] Potential butyrate producer based on taxa [106]
Rikenellaceae AF12 (Millionella massiliensis) (ASV_344)	B A I	Late, Post Pre-Late/Post Pre, Early-Mid	**Butyrate** producer associated with exercise [113]
Alphaproteobacteria RF32 (Kiloniella laminariae) (ASV_474)[3]	B I M[4]	Late, Post Early-Mid, Post Post	Colonic damage [139], inverse with 5-HT [140]
Lachnospiraceae (*Clostridium colinum*) (ASV_399)	M	Late, All	Potential **butyrate**, and Indoleacrylic acid producer based

			on taxa [106, 133, 141]
Coprobacillus (Longibaculum muris) (ASV_350)	M	Late	Positively correlated with leptin (anti-obesity) [142]
Blautia (*Murimonas intestini*) (ASV_398)[3]	B A I	Late, Post Early-Post Post	Acetate producer (Potential co-metabolism feeding for **butyrate** producers), inversely correlated with PD [112] Linked to gut homeostasis [130, 143]
Staphylococcus (Staphylococcus saprophyticus) (ASV_519)	A	Late	Grooming [144]
Candidatus Anthromitus (Clostridium oryzae) (ASV_427)	M	Late, Post	Potential **butyrate** producer based on taxa [105, 106] Linked to inflammation [145] Controversial taxonomic assignment [146, 147]
Anaerofustis (Anaerofustis stercorihominis) (ASV_779)	B I M	Combined Post Early, Late, Post, All	Acetate and **butyrate** [148]
TM7 F16 (Geomonas terrae) (ASV_1026)[3]	I	Early-Mid, Post	Associated with gut dysbiosis and inflammation [149, 150]
Cupriavidus (Cupriavidus metallidurans) (ASV_836)	M	Early, Late	Environmental contaminant [151]
Pseudomonas (Pseudomonas aeruginosa) (ASV_71)	M	Early	Becomes more virulent in the presence of morphine [152]
Papillibacter (Clostridium viride)(ASV_3108)	M	Late, Post	Potential **butyrate** producer based on taxa [105, 106]
Burkholderia (Burkholderia territorii) (ASV_1302)[3]	I	Early	Potential pathogen [153, 154]
Xanthomonas (Xanthomonas albilineans) (ASV_2124)3	I	Early-Mid	Participate in bile acid metabolism [155, 156]
Stenotrophomonas (Xanthomonas floridensis)(ASV_7876)3*	I	Post	Associated with gut inflammation [157, 158]

[1] Ordered by decreasing abundance. Species (in parentheses) were identified using rRNA/ITS databases with the nucleotide basic local alignment search tool (blastn) [66].
[2] B: Biomarker of non-tolerance; A: High starting antinociception; I: Indicator taxa of non-tolerance; M: Predictive modelling.
[3] Altered by morphine exposure
[4] Identified in predictive models for both tolerance and non-tolerant mice but in combination with different taxa

FIGURE CAPTIONS

Figure 1: Natural variability in antinociceptive tolerance to chronic morphine does not correlate with the amount of morphine mice voluntarily consumed. A) Mouse (n=16) chronic morphine oral self-administration paradigm where voluntary morphine consumption was monitored[53]. Fecal samples were collected during each phase of morphine experience and used to generate16S (V4-V5 region, see methods) microbiota for analysis. B) Linear regression of total morphine consumption with degree of tolerance showing lack of correlation (y = 78 - 0.16x; R2 = -0.14; Pearson's correlation p-value = 0.61). C) Morphine antinociception (6 mg/kg sub-cutaneous, ED_{80}) was determined at the start of study and post-chronic morphine (week 19) using a radiant tail flick assay to determine tolerance to morphine. Data is reported as maximum possible effect (% MPE). Colored individuals exhibited low starting antinociception which decreased further after chronic morphine consumption. D) Pre-morphine gut microbiota β-diversity (Bray-Curtis dissimilarity) was visualized by principal coordinates analysis (PCoA). See Supplemental Table 1 for details.

Figure 2: Chronic morphine induced predictive dysbiosis in all mice. A) Temporal changes in gut microbiota β-diversity (All ASVs, Bray-Curtis dissimilarity) as visualized by principal coordinates analysis (PCoA). See Supplemental Table 1 for details. B) Comparison of bacterial association networks before (left) and after 18 weeks (right) of oral morphine using the SPRING method in NetCoMi [90]. Edges are colored by sign (positive: green, negative: red), representing estimated associations between community members. *Adlercreutzia* (ASV_166) and *Streptococcus* (ASV_869) are the only two community members identified as hubs (bolded text and borders). Eigenvector centrality was used for scaling node sizes and colors representing clusters of genera (determined using greedy modularity optimization). Clusters have the same color in both networks if they share at least two taxa. Nodes that are not connected in both

groups were excluded. Corresponding taxa names detailed in Supplemental Table 4. C) Predictive modelling of morphine exposed microbiota (using R program indicspecies) [86]. β-diversity (All ASVs, Bray-Curtis dissimilarity) as visualized by principal coordinates analysis (PCoA) demonstrates the starting composition of microbiota of mice that trained the models (JAX-bred, orange triangles), which group in the lower right corner, and of mice that tested the models (home-bred, orange circles), which group in the upper right corner, differ but converge during and after morphine exposure. The right bar graphs show % accuracy of the models to predict whether microbiota from home-bred mice resulted from morphine exposure (as % correct/incorrect). See supplemental Tables 4 and 5 for details.

Figure 3: Morphine led to concurrent increase in pathobionts and decrease in mutualists that produce SCFAs. A) Biomarkers of morphine consumption were identified from among the community members whose abundance was significantly altered by morphine (37 species, ~21% of taxa) using corncob binomial regression models [84], followed by a linear discrimination analysis (LDA) of effect size (LEfSe) [85]. Asterisks indicate where in the paradigm the community member was a biomarker. Community members are labeled at the lowest taxonomic classification available. See Supplemental Table 2 for details. B) Functions of the microbiota whose abundance was differentially abundant during and after morphine exposure relative to their starting abundances were inferred from published studies (See Supplemental Table 7), which indicated that morphine exposure resulted in concurrent depletion of SCFA-producing genera and proliferation of pathobionts. Figure created with BioRender.com.

Figure 4: Analysis of differential responses of the microbiota to morphine disturbance reveal microbiota associations with variability of tolerance. A) Change in average microbiota α-alpha diversity at the genus level is plotted sequentially by sample number for

tolerant (grey line) and non-tolerant (black line) mice, assessed using number and evenness of species (Shannon). Bayesian change-points in diversity of tolerant (grey star) and non-tolerant (black star) mice are shown. Error bars represent SEM. B) Biomarkers of antinociceptive tolerance to chronic morphine were identified from among the community members whose abundance was explained by tolerance (as identified using corncob regression models) [84], followed by a linear discrimination analysis (LDA) of effect size (LEfSe) [85] representing genera that most likely explain differences between the microbiota of tolerant (poppy symbol) or non-tolerant mice (asterisk). Community members are labeled at the genus level or at the lowest taxonomic classification available when genus was not available. *Desulfovibrio*, *Odoribacter*, and *Anaerofustis* were only identified as biomarkers when microbiomes from all experiences were combined. See Supplemental Table 9 for details. C) Temporal stability of the gut microbiota of individual mice at each phase of morphine experience was assessed by analysis of Type IV Taylor's Power Law parameters [88] [89]. The average slope parameter for each mouse at each phase of morphine exposure was normalized by subtracting the average pre-morphine slope parameter. Positively increasing average change in slope (black line with grey confidence intervals) represents microbiota instability and displayed by tolerant mice. See methods for details and Supplemental Figure 9 for Type I analysis showing aggregation at all phases representing normal stochasticity. D) Differences in network associations between non-tolerant and tolerant mice. Associations of genera that were different between tolerant and non-tolerant mice, extracted from Supplemental Figure 10 are represented by a connecting line where colors indicate positive or negative associations and thickness indicates relative difference in strength of connection between non-tolerant and tolerant mice. See Supplemental Table 10 for statistics.

Figure 5: Summary of genera informing predictive models exemplifying more stable associations and shared predictive genera among non-tolerant than tolerant mice. Summary of taxa used in combinations to predict whether a microbiota sample was from a tolerant mouse (red) or a non-tolerant mouse (blue) in different phases of morphine experience. No models were predictive during pre-morphine. Three genera that were inconsistently identified in biomarker, indicator, or network analyses (showing the opposite associations in prior analyses at the same phase of morphine experience compared to these models) were excluded from this visual summary. See Supplemental Table 11 & 12 for details.

Figure 6: **Butyrate supplementation prolongs morphine antinociception**. A) Schematic of mouse paradigm where mice were fed 100 mM sodium butyrate or sodium citrate, followed either by 9-days morphine (10 mg/kg s.c.) (n = 18 ea), or daily saline (0.9% s.c.) (n = 8 ea). Morphine treatment mice were assessed for baseline nociception and morphine antinociception on Day 1, 7, and 10 at 5mg/kg and 30 minutes later at 5+2 mg/kg s.c. morphine (ED_{60} and ED_{90} respectively, see Supplemental Figure 13B). The trajectory of tolerance to morphine was visualized as a decrease in latency to tail-flick (s) (5 + 2 mg/kg s.c. morphine) and reported as mean; error bars are SEM. Kruskal-Wallis test followed by pairwise Wilcox test with corrections for multiple comparisons were used to determine whether citrate and butyrate groups changed over time (horizontal error bars) and differed from each other (asterisks above data points) (*P<0.05; **P<0.01; ***P<0.001). C) Morphine antinociception (5 + 2 mg/kg s.c. morphine) as determined on day 10 using the radiant tail flick assay. Data is reported as maximum possible effect (% MPE). Kruskal-Wallis test followed by pairwise Wilcox test for multiple comparisons determined significant differences between morphine treated citrate and butyrate supplementation groups and between morphine treatments and saline controls (**P<0.01; ***P<0.001). D) Tolerance was assessed by comparison of linear regressions of dose responses (ED_{60} and ED_{80} doses) reported as %MPE on Day 1 (open squares) and Day 10

(closed squares). Outer dashed lines represent 95% confidence intervals of the linear regressions and error bars represent SEM. Shift in ED_{50} from Day 1 to Day 8 extrapolated from these regressions is reported in text.

Figure 7: Simplified models of microbiota protection from antinociceptive tolerance to morphine by sustained production of butyrate. The reduction of SCFAs, notably butyrate, and increase in pro-inflammatory cytokines combined with prolonged morphine stimulation of MOR expressed on neurons, drives homeostatic adaptations that manifest as tolerance (See Supplemental Figure 1 and 2 for mechanistic details). Sustained production of neuroactive butyrate by diverse bacteria improves gut barrier function, attenuates inflammation, promotes clearing of commensals that breach the barrier thereby countering progressing dysbiosis under the pressure of morphine disruption (left panels)(mechanistic details described in Supplemental Figure 14). Butyrate could prevent or delay homeostatic changes in MOR-expressing neurons in response to chronic morphine even independently of its effects on inflammation as a ligand to Gi-protein coupled receptors expressed on sensory neurons to dampen their increased excitability or change release of neurotransmitters (right panels).

Figure 1

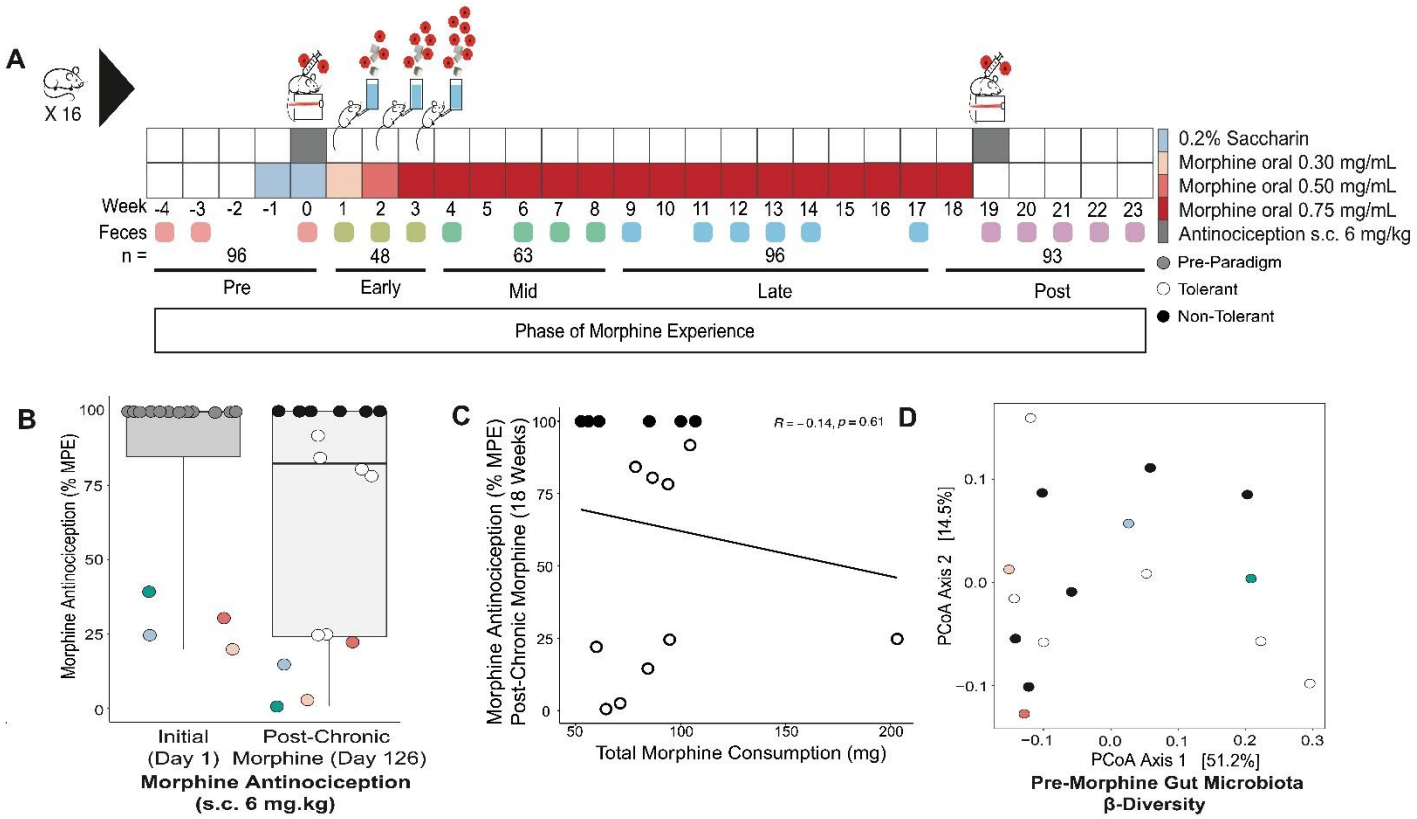
A
X 16
Week -4 -3 -2 -1 0 1 2 3 4 5 6 7 8 9 10 11 12 13 14 15 16 17 18 19 20 21 22 23
Feces
n = 96 48 63 96 93
Pre
Early
Mid
Late
Post
Phase of Morphine Experience
0.2% Saccharin
Morphine oral 0.30 mg/mL
Morphine oral 0.50 mg/mL
Morphine oral 0.75 mg/mL
Antinociception s.c. 6 mg/kg
Pre-Paradigm
Tolerant
Non-Tolerant
B
Morphine Antinociception (% MPE)
Initial (Day 1)
Post-Chronic Morphine (Day 126)
Morphine Antinociception (s.c. 6 mg.kg)
C
Morphine Antinociception (% MPE) Post-Chronic Morphine (18 Weeks)
R = −0.14, p = 0.61
Total Morphine Consumption (mg)
D
PCoA Axis 2 [14.5%]
PCoA Axis 1 [51.2%]
Pre-Morphine Gut Microbiota β-Diversity

Figure 2

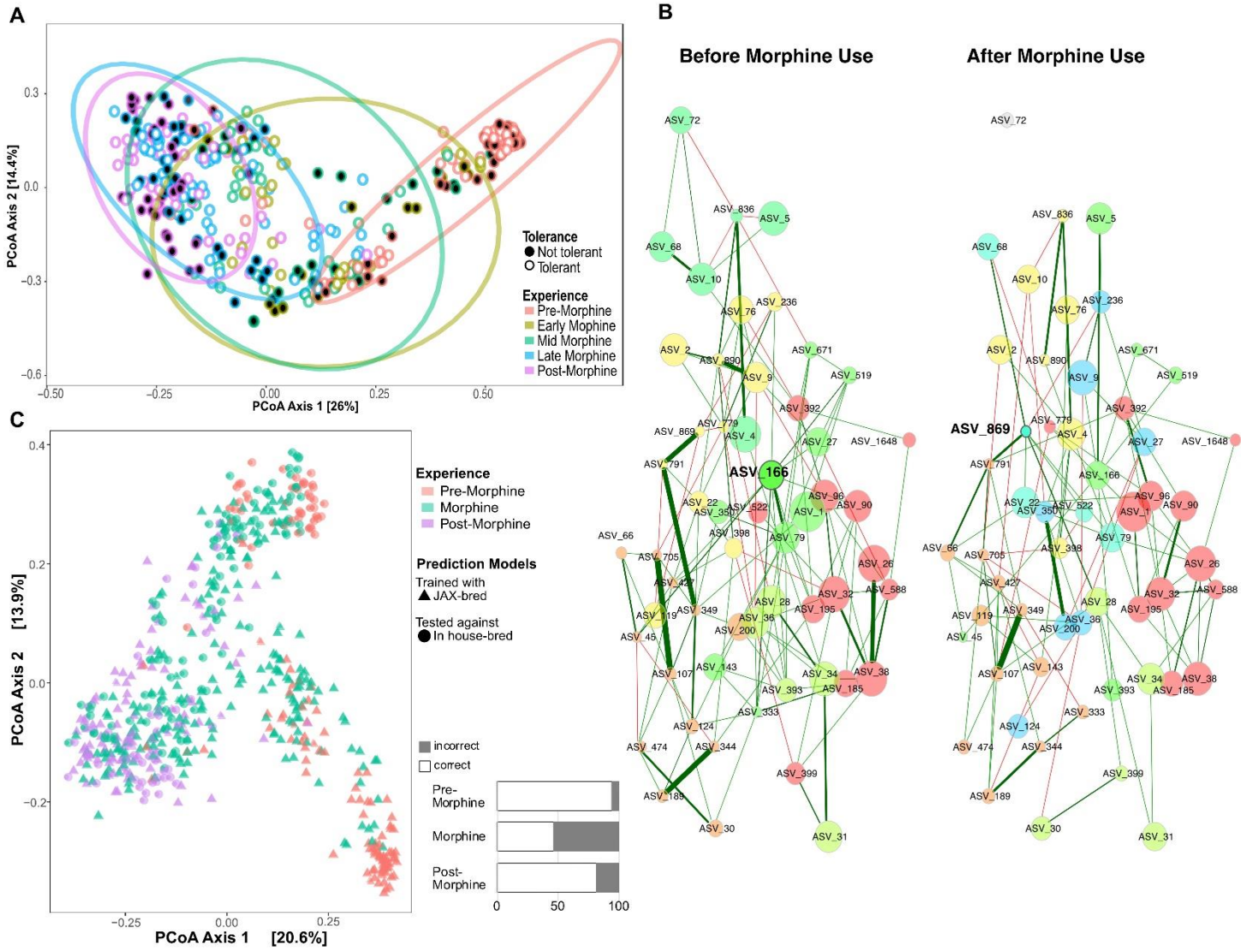
A
PCoA Axis 2 [14.4%]
PCoA Axis 1 [26%]
Tolerance
Not tolerant
Tolerant
Experience
Pre-Morphine
Early Mophine
Mid Morphine
Late Morphine
Post-Morphine
B
Before Morphine Use
After Morphine Use
ASV_166
ASV_869
C
PCoA Axis 2 [13.9%]
PCoA Axis 1 [20.6%]
Experience
Pre-Morphine
Morphine
Post-Morphine
Prediction Models
Trained with
JAX-bred
Tested against
In house-bred
incorrect
correct
Pre-Morphine
Morphine
Post-Morphine

Figure 3

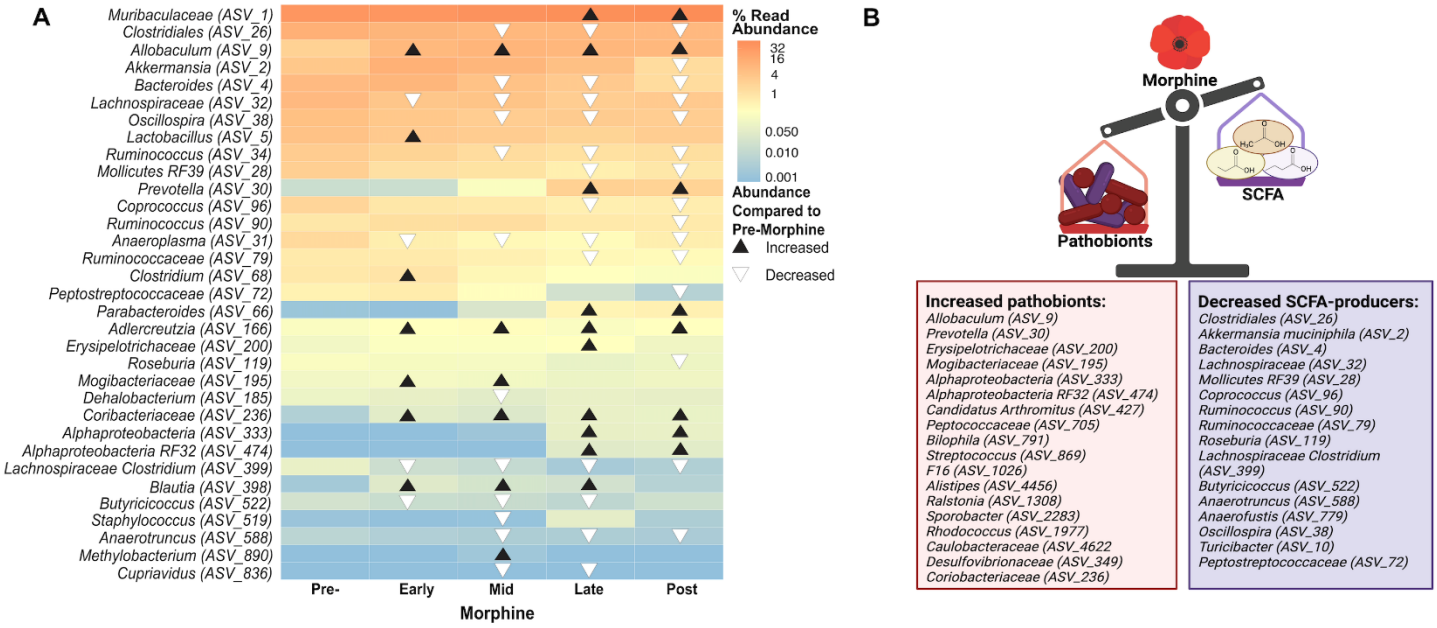
A
Muribaculaceae (ASV_1)
Clostridiales (ASV_26)
Allobaculum (ASV_9)
Akkermansia (ASV_2)
Bacteroides (ASV_4)
Lachnospiraceae (ASV_32)
Oscillospira (ASV_38)
Lactobacillus (ASV_5)
Ruminococcus (ASV_34)
Mollicutes RF39 (ASV_28)
Prevotella (ASV_30)
Coprococcus (ASV_96)
Ruminococcus (ASV_90)
Anaeroplasma (ASV_31)
Ruminococcaceae (ASV_79)
Clostridium (ASV_68)
Peptostreptococcaceae (ASV_72)
Parabacteroides (ASV_66)
Adlercreutzia (ASV_166)
Erysipelotrichaceae (ASV_200)
Roseburia (ASV_119)
Mogibacteriaceae (ASV_195)
Dehalobacterium (ASV_185)
Coribacteriaceae (ASV_236)
Alphaproteobacteria (ASV_333)
Alphaproteobacteria RF32 (ASV_474)
Lachnospiraceae Clostridium (ASV_399)
Blautia (ASV_398)
Butyricicoccus (ASV_522)
Staphylococcus (ASV_519)
Anaerotruncus (ASV_588)
Methylobacterium (ASV_890)
Cupriavidus (ASV_836)
Pre-
Early
Mid
Late
Post
Morphine
% Read Abundance
32
16
4
1
0.050
0.010
0.001
Abundance Compared to Pre-Morphine
Increased
Decreased
B
Morphine
Pathobionts
SCFA
Increased pathobionts:
Allobaculum (ASV_9)
Prevotella (ASV_30)
Erysipelotrichaceae (ASV_200)
Mogibacteriaceae (ASV_195)
Alphaproteobacteria (ASV_333)
Alphaproteobacteria RF32 (ASV_474)
Candidatus Arthromitus (ASV_427)
Peptococcaceae (ASV_705)
Bilophila (ASV_791)
Streptococcus (ASV_869)
F16 (ASV_1026)
Alistipes (ASV_4456)
Ralstonia (ASV_1308)
Sporobacter (ASV_2283)
Rhodococcus (ASV_1977)
Caulobacteraceae (ASV_4622
Desulfovibrionaceae (ASV_349)
Coriobacteriaceae (ASV_236)
Decreased SCFA-producers:
Clostridiales (ASV_26)
Akkermansia muciniphila (ASV_2)
Bacteroides (ASV_4)
Lachnospiraceae (ASV_32)
Mollicutes RF39 (ASV_28)
Coprococcus (ASV_96)
Ruminococcus (ASV_90)
Ruminococcaceae (ASV_79)
Roseburia (ASV_119)
Lachnospiraceae Clostridium (ASV_399)
Butyricicoccus (ASV_522)
Anaerotruncus (ASV_588)
Anaerofustis (ASV_779)
Oscillospira (ASV_38)
Turicibacter (ASV_10)
Peptostreptococcaceae (ASV_72)

Figure 4

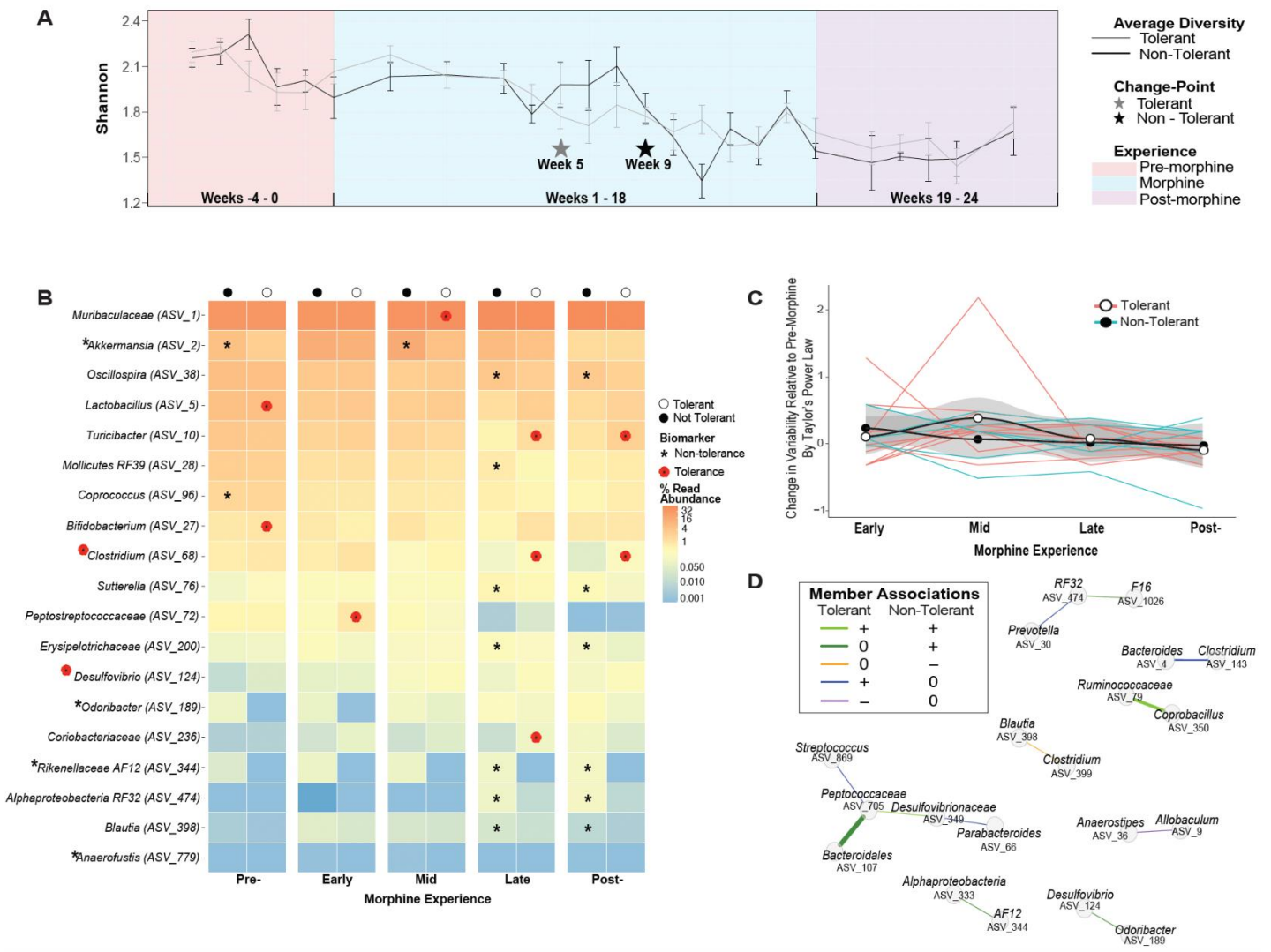
A
Shannon
2.4
2.1
1.8
1.5
1.2
Week 5
Week 9
Weeks -4 - 0
Weeks 1 - 18
Weeks 19 - 24
Average Diversity
Tolerant
Non-Tolerant
Change-Point
Tolerant
Non - Tolerant
Experience
Pre-morphine
Morphine
Post-morphine
B
Muribaculaceae (ASV_1)
*Akkermansia (ASV_2)
Oscillospira (ASV_38)
Lactobacillus (ASV_5)
Turicibacter (ASV_10)
Mollicutes RF39 (ASV_28)
Coprococcus (ASV_96)
Bifidobacterium (ASV_27)
Clostridium (ASV_68)
Sutterella (ASV_76)
Peptostreptococcaceae (ASV_72)
Erysipelotrichaceae (ASV_200)
Desulfovibrio (ASV_124)
*Odoribacter (ASV_189)
Coriobacteriaceae (ASV_236)
*Rikenellaceae AF12 (ASV_344)
Alphaproteobacteria RF32 (ASV_474)
Blautia (ASV_398)
*Anaerofustis (ASV_779)
Pre-
Early
Mid
Late
Post-
Morphine Experience
Tolerant
Not Tolerant
Biomarker
Non-tolerance
Tolerance
% Read Abundance
32
16
4
1
0.050
0.010
0.001
C
Change in Variability Relative to Pre-Morphine By Taylor's Power Law
Tolerant
Non-Tolerant
Early
Mid
Late
Post-
Morphine Experience
D
Member Associations
Tolerant
Non-Tolerant
RF32 ASV_474
F16 ASV_1026
Prevotella ASV_30
Bacteroides ASV_4
Clostridium ASV_143
Ruminococcaceae ASV_79
Coprobacillus ASV_350
Blautia ASV_398
Streptococcus ASV_869
Clostridium ASV_399
Peptococcaceae ASV_705
Desulfovibrionaceae ASV_349
Parabacteroides ASV_66
Anaerostipes ASV_36
Allobaculum ASV_9
Bacteroidales ASV_107
Alphaproteobacteria ASV_333
Desulfovibrio ASV_124
AF12 ASV_344
Odoribacter ASV_189

Figure 5

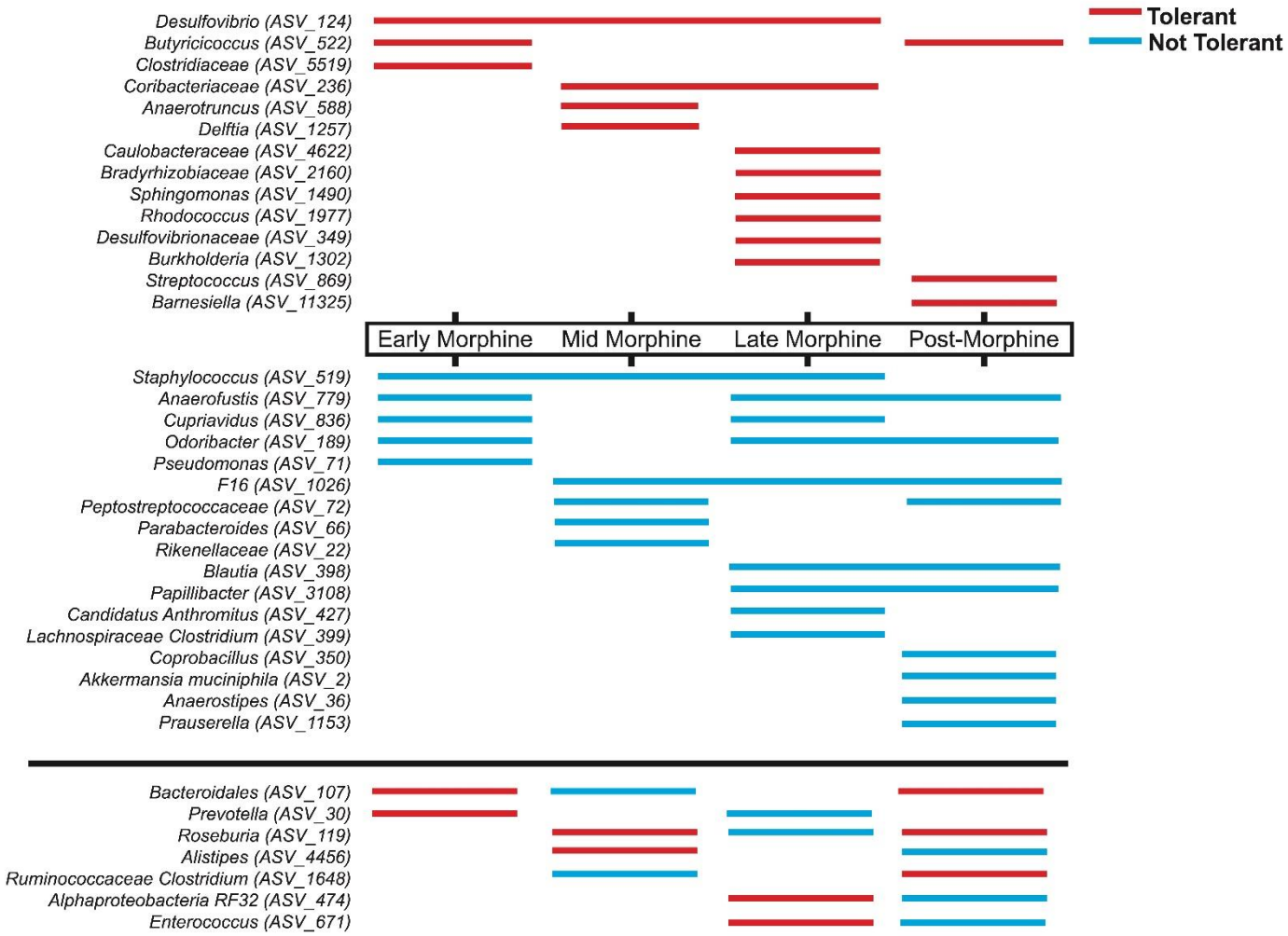
Tolerant
Not Tolerant
Desulfovibrio (ASV_124)
Butyricicoccus (ASV_522)
Clostridiaceae (ASV_5519)
Coribacteriaceae (ASV_236)
Anaerotruncus (ASV_588)
Delftia (ASV_1257)
Caulobacteraceae (ASV_4622)
Bradyrhizobiaceae (ASV_2160)
Sphingomonas (ASV_1490)
Rhodococcus (ASV_1977)
Desulfovibrionaceae (ASV_349)
Burkholderia (ASV_1302)
Streptococcus (ASV_869)
Barnesiella (ASV_11325)
Early Morphine
Mid Morphine
Late Morphine
Post-Morphine
Staphylococcus (ASV_519)
Anaerofustis (ASV_779)
Cupriavidus (ASV_836)
Odoribacter (ASV_189)
Pseudomonas (ASV_71)
F16 (ASV_1026)
Peptostreptococcaceae (ASV_72)
Parabacteroides (ASV_66)
Rikenellaceae (ASV_22)
Blautia (ASV_398)
Papillibacter (ASV_3108)
Candidatus Anthromitus (ASV_427)
Lachnospiraceae Clostridium (ASV_399)
Coprobacillus (ASV_350)
Akkermansia muciniphila (ASV_2)
Anaerostipes (ASV_36)
Prauserella (ASV_1153)
Bacteroidales (ASV_107)
Prevotella (ASV_30)
Roseburia (ASV_119)
Alistipes (ASV_4456)
Ruminococcaceae Clostridium (ASV_1648)
Alphaproteobacteria RF32 (ASV_474)
Enterococcus (ASV_671)

Figure 6

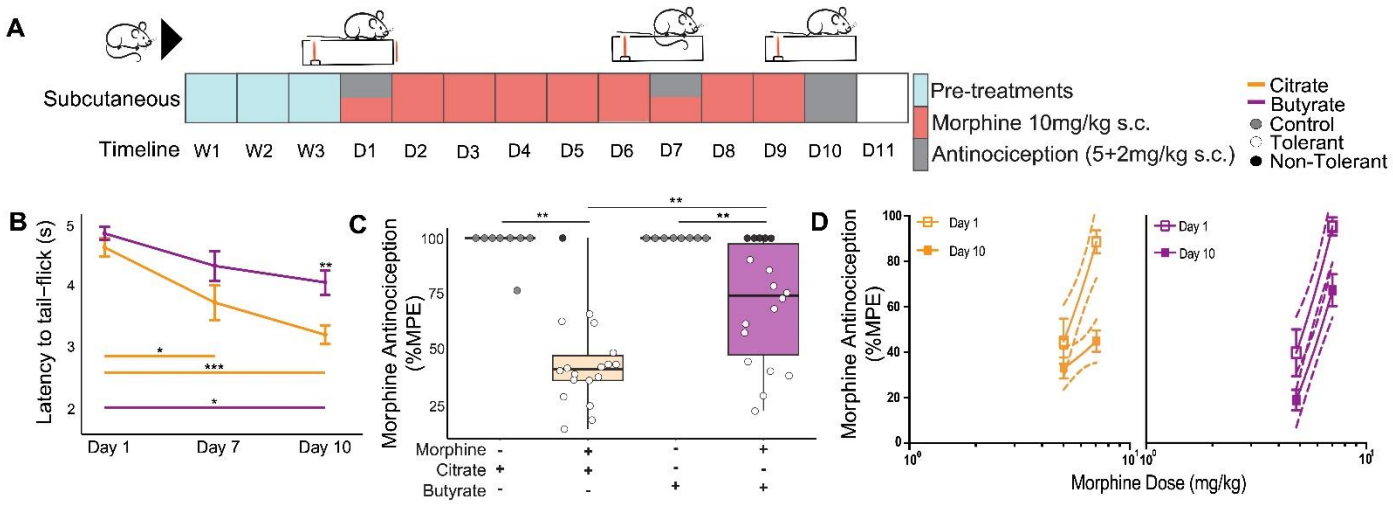
A
Subcutaneous
Timeline W1 W2 W3 D1 D2 D3 D4 D5 D6 D7 D8 D9 D10 D11
Pre-treatments
Morphine 10mg/kg s.c.
Antinociception (5+2mg/kg s.c.)
Citrate
Butyrate
Control
Tolerant
Non-Tolerant
B
Latency to tail-flick (s)
Day 1
Day 7
Day 10
C
Morphine Antinociception (%MPE)
Morphine
Citrate
Butyrate
D
Morphine Antinociception (%MPE)
Day 1
Day 10
Morphine Dose (mg/kg)

Figure 7

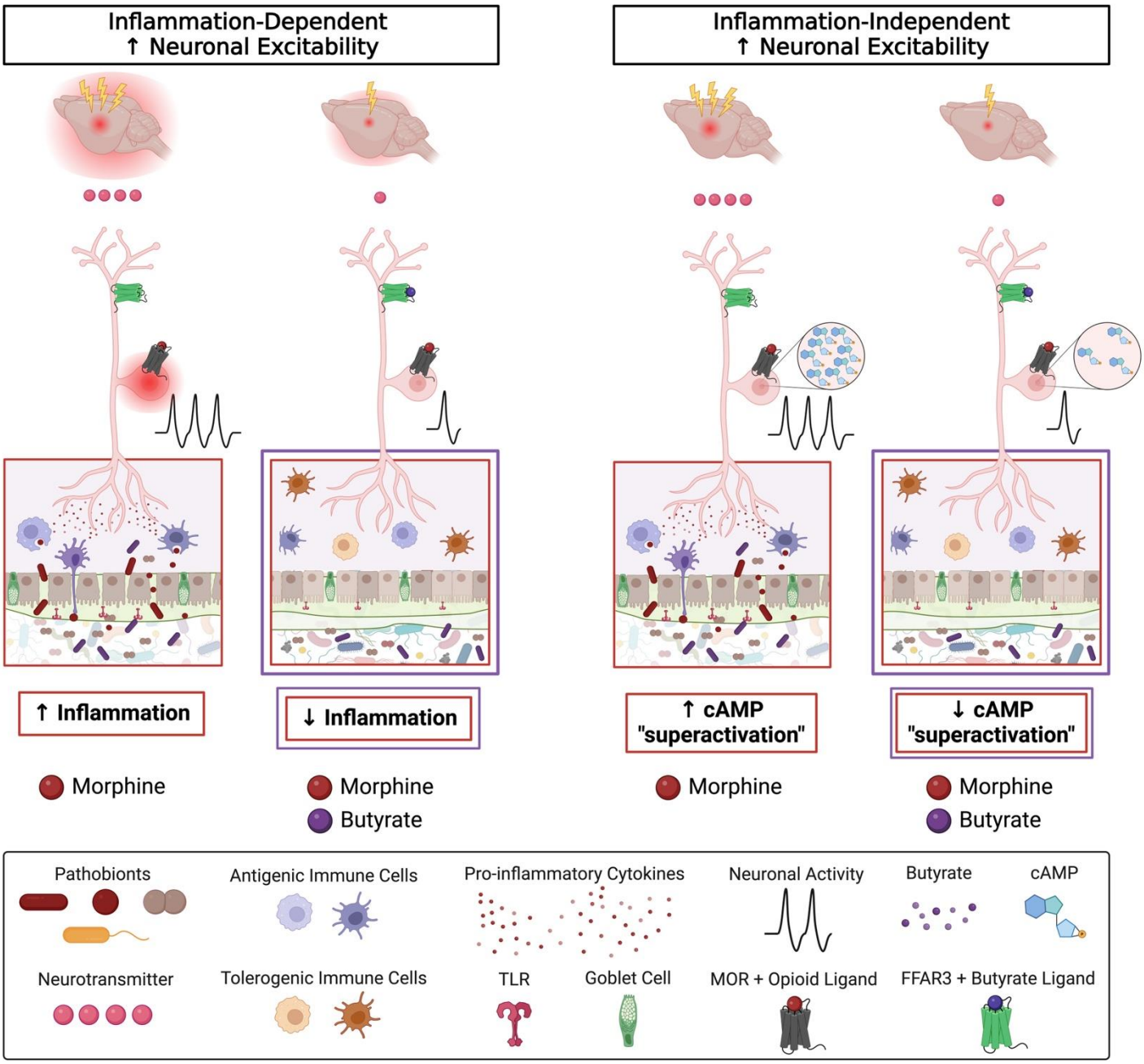
Inflammation-Dependent
↑ Neuronal Excitability
Inflammation-Independent
↑ Neuronal Excitability
↑ Inflammation
↓ Inflammation
↑ cAMP
"superactivation"
↓ cAMP
"superactivation"
Morphine
Morphine
Butyrate
Morphine
Morphine
Butyrate
Pathobionts
Antigenic Immune Cells
Pro-inflammatory Cytokines
Neuronal Activity
Butyrate
cAMP
Neurotransmitter
Tolerogenic Immune Cells
TLR
Goblet Cell
MOR + Opioid Ligand
FFAR3 + Butyrate Ligand